



Skew-symmetric form of convective terms and fully conservative finite difference schemes for variable density low-Mach number flows

Yohei Morinishi *

Graduate School of Engineering, Nagoya Institute of Technology, Gokiso-cho, Showa-ku, Nagoya 466-8555, Japan

ARTICLE INFO

Article history:

Received 26 May 2009

Received in revised form 11 September 2009

Accepted 21 September 2009

Available online 9 October 2009

Keywords:

Convective term

Compressible flow

Skew-symmetric form

Divergence form

Advective form

Finite difference

Compact finite difference

Fully conservative

Secondary conservative

Staggered grid system

Regular grid system

ABSTRACT

The form of convective terms for compressible flow equations is discussed in the same way as for an incompressible one by Morinishi et al. [Y. Morinishi, T.S. Lund, O.V. Vasilyev, P. Moin, Fully conservative higher order finite difference schemes for incompressible flow, *J. Comput. Phys.* 124 (1998) 90], and fully conservative finite difference schemes suitable for shock-free unsteady compressible flow simulations are proposed. Commutable divergence, advective, and skew-symmetric forms of convective terms are defined by including the temporal derivative term for compressible flow. These forms are analytically equivalent if the continuity is satisfied, and the skew-symmetric form is secondary conservative without the aid of the continuity, while the divergence form is primary conservative. The relations between the present and existing quasi-skew-symmetric forms are also revealed. Commutable fully discrete finite difference schemes of convection are then derived in a staggered grid system, and they are fully conservative provided that the corresponding discrete continuity is satisfied. In addition, a semi-discrete convection scheme suitable for compact finite difference is presented based on the skew-symmetric form. The conservation properties of the present schemes are demonstrated numerically in a three-dimensional periodic inviscid flow. The proposed fully discrete fully conservative second-order accurate scheme is also used to perform the DNS of compressible isotropic turbulence and the simulation of open cavity flow.

© 2009 Elsevier Inc. All rights reserved.

1. Introduction

The fully conservative finite difference scheme is recognized as a useful tool for unsteady turbulence simulations like DNS and LES, since it is free of numerical dissipation and offers stable long-term integration. The scheme is composed of a proper set of discrete governing equations for incompressible flow as shown in Morinishi et al. [1]. In particular, the finite difference for the convective term is one of commutable convection schemes for divergence, advective, and skew-symmetric forms, which are equivalent if the corresponding discrete continuity is satisfied. In addition, the schemes for divergence and skew-symmetric forms have primary and secondary conservation properties, respectively, without the aid of the continuity. Here, the secondary or quadratic conservation property is the property with which the quadratic quantity of a transport variable is conserved, while the primary conservation or merely conservation property is the one for the standard conservation form. For instance, the continuity is the primary mass conservation equation, and the kinetic energy is the quadratic quantity of momentum. Therefore, the fully conservative finite difference scheme for incompressible flow conserves momentum and kinetic energy simultaneously in the inviscid limit as long as the discrete continuity is satisfied. The convection scheme in

* Corresponding author. Tel.: +81 52 735 5346; fax: +81 52 735 5342.

E-mail address: morinishi.yohei@nitech.ac.jp.

the original staggered method by Harlow and Welch [2] was one of the fully conservative second-order accurate convection schemes. Fourth and higher order accurate schemes were proposed by Morinishi et al. [1]. Vasilyev [3] extended the fourth-order scheme to non-uniform meshes by introducing mesh mapping, although his method had commutation error and was not fully conservative. Fully conservative high-order accurate schemes in a non-uniform cylindrical coordinate system were derived by Morinishi et al. [4]. The fourth-order convection scheme by Verstappen and Veldman [5] is not fully but secondary conservative.

Extension to compressible flow has been attempted by some researchers. For instance, Nicoud [6] simply extended the fourth-order accurate incompressible convection schemes by Morinishi et al. [1] to compressible ones. Desjardins et al. [7] extended the high-order accurate cylindrical method by Morinishi et al. [4] to compressible flow. Actually, the convection schemes for divergence and advective forms corresponding to those in Nicoud [6] and Desjardins et al. [7] are semi-discrete fully conservative schemes for compressible flow. It is known that the skew-symmetric form has a role of de-aliasing [8,9], and some skew-symmetric like forms, called quasi-skew-symmetric forms in this study, were used for unsteady compressible flow simulations [10–15]. However, no convection scheme of skew-symmetric form which is secondary conservative for compressible flow has been proposed so far. This is due to the lack of knowledge of commutable convection forms for compressible flow equations.

For variable density low-Mach number flow simulations, an implicit time marching method is preferred due to severe stability restriction by the acoustic velocity. For incompressible flow, a fully (spatio-temporal) discrete fully conservative method was constructed by Ham et al. [16] with an implicit mid-point time marching method. Pierce et al. [17] and Wall et al. [18] have tried to construct a fully discrete fully conservative scheme for compressible flow, their convection schemes, however, have temporal second-order error about the secondary conservation.

In this study, the form of convective terms for compressible flow equations is discussed in the same way as for an incompressible one by Morinishi et al. [1], and fully conservative finite difference schemes suitable for shock-free unsteady compressible flow simulations are proposed. The paper is organized as follows. Forms of convective terms for compressible flow equations are analyzed in Section 2. Conservation properties of mass, momentum, and energy equations are reviewed in Section 3. These conservation properties are regarded as analytical requirements for a proper set of discrete equations for compressible flow. In Section 4, fully discrete fully conservative finite difference schemes for variable density low-Mach number flows are proposed in a staggered grid system. Semi-discrete convection schemes with the standard and compact finite differences are also discussed in Section 5. Numerical tests are performed in Section 6. For the reader's convenience, schemes in a regular grid system are presented in Appendix A, and a non-uniform grid arrangement of the fully discrete fully conservative finite difference scheme in a staggered grid system is presented in Appendix B.

2. Forms of convective terms for transport equations of compressible flow

The transport equations of conserved variables for compressible flow are in general cast into the conservative form.

$$\frac{\partial \rho \phi}{\partial t} + \frac{\partial \rho u_j \phi}{\partial x_j} = \frac{\partial F_{\phi j}}{\partial x_j}. \tag{1}$$

In this equation t is time, $x_i (i = 1, 2, 3)$ are spatial coordinates, ρ is density, u_i are the components of velocity vector, and $F_{\phi j}$ are the components of flux for ϕ . Repeated indices of vector and tensor components follow the summation convention. The physical meaning of the term “conservative form” comes from the nature of (1). Applying Gauss' divergence theorem to (1) yields

$$\frac{d}{dt} \int_V (\rho \phi) dV = \int_S (F_{\phi j} - \rho u_j \phi) n_j dS, \tag{2}$$

where S is the surface area surrounding volume V , and n_j is the outward surface normal. For compressible flow, the sum of the density weighted variable $(\rho \phi)$ in the volume is conserved in time if the sum of the flux $(F_{\phi j} - \rho u_j \phi) n_j$ through the surface has disappeared. This means that $(\rho \phi)$ in the volume is conserved in time for periodic or flux-free flows if the transport equation is written in the conservative form. The form of convective terms in (1) is called divergence form. On the other hand, the left-hand side of (1) is sometimes rewritten into the following form:

$$\rho \frac{\partial \phi}{\partial t} + \rho u_j \frac{\partial \phi}{\partial x_j} = \frac{\partial F_{\phi j}}{\partial x_j}. \tag{3}$$

The latter is equivalent to the former with the aid of the continuity,

$$\frac{\partial \rho}{\partial t} + \frac{\partial \rho u_j}{\partial x_j} = 0. \tag{4}$$

The equivalence, however, is not always valid for a discrete counterpart. For incompressible flow, some special finite difference schemes hold the equivalence and also secondary conservation property and are suitable for unsteady turbulent flow simulations. In this study, the form of the convective term for compressible flow equations is investigated in the same manner as for an incompressible one by Morinishi et al. [1]. That is, the left-hand side of the continuity, $(Cont.)$, and the divergence and advective forms of convective terms, $(Div.)_\phi$ and $(Adv.)_\phi$, are respectively defined as

$$(\text{Cont.}) \equiv \frac{\partial \rho}{\partial t} + \frac{\partial \rho u_j}{\partial x_j} (= 0), \quad (5)$$

$$(\text{Div.})_\phi \equiv \frac{\partial \rho \phi}{\partial t} + \frac{\partial \rho u_j \phi}{\partial x_j}, \quad (6)$$

$$(\text{Adv.})_\phi \equiv \rho \frac{\partial \phi}{\partial t} + \rho u_j \frac{\partial \phi}{\partial x_j}. \quad (7)$$

Note that the temporal derivative term is included in each definition because of the equivalence through the continuity:

$$(\text{Div.})_\phi = (\text{Adv.})_\phi + \phi (\text{Cont.}). \quad (8)$$

Then, the skew-symmetric form is defined as the arithmetic average of the divergence and advective forms:

$$(\text{Skew.})_\phi \equiv \frac{1}{2}(\text{Div.})_\phi + \frac{1}{2}(\text{Adv.})_\phi = (\text{Div.})_\phi - \frac{1}{2}\phi (\text{Cont.}) = (\text{Adv.})_\phi + \frac{1}{2}\phi (\text{Cont.}). \quad (9)$$

Consequently, the divergence, advective and skew-symmetric forms are equivalent if $(\text{Cont.}) = 0$, and there are only two independent convection forms. The arithmetic average directly gives one of the skew-symmetric forms:

$$\frac{1}{2}(\text{Div.})_\phi + \frac{1}{2}(\text{Adv.})_\phi = \frac{1}{2} \left(\frac{\partial \rho \phi}{\partial t} + \rho \frac{\partial \phi}{\partial t} \right) + \frac{1}{2} \left(\frac{\partial \rho u_j \phi}{\partial x_j} + \rho u_j \frac{\partial \phi}{\partial x_j} \right).$$

However, the skew-symmetric form above contains multiple temporal derivative terms and seems too difficult to integrate in time with an explicit time marching method. Fortunately, the following transformations reveal the existence of useful skew-symmetric forms:

$$\frac{1}{2} \left(\frac{\partial \rho \phi}{\partial t} + \rho \frac{\partial \phi}{\partial t} \right) = \left(\frac{\partial \rho \phi}{\partial t} - \frac{\phi}{2} \frac{\partial \rho}{\partial t} \right) = \left(\rho \frac{\partial \phi}{\partial t} + \frac{\phi}{2} \frac{\partial \rho}{\partial t} \right) = \sqrt{\rho} \frac{\partial \sqrt{\rho} \phi}{\partial t}, \quad (10)$$

$$\frac{1}{2} \left(\frac{\partial \rho u_j \phi}{\partial x_j} + \rho u_j \frac{\partial \phi}{\partial x_j} \right) = \left(\frac{\partial \rho u_j \phi}{\partial x_j} - \frac{\phi}{2} \frac{\partial \rho u_j}{\partial x_j} \right) = \left(\rho u_j \frac{\partial \phi}{\partial x_j} + \frac{\phi}{2} \frac{\partial \rho u_j}{\partial x_j} \right) = \sqrt{\rho u_j} \frac{\partial \sqrt{\rho u_j} \phi}{\partial x_j}, \quad (11)$$

where $\sqrt{\rho u_j} \frac{\partial \sqrt{\rho u_j} \phi}{\partial x_j} \equiv \sum_{j=1}^3 \sqrt{\rho u_j} \frac{\partial \sqrt{\rho u_j} \phi}{\partial x_j}$ for three-dimensional problems. The last representation in (11) is available if complex number can be handled. It is apparent from (10) and (11) that there are at least sixteen variants of the skew-symmetric form. In this study, the canonical form of the skew-symmetric form which is secondary conservative *a priori* is selected from among the sixteen variants as

$$(\text{Skew.})_\phi \equiv \sqrt{\rho} \frac{\partial \sqrt{\rho} \phi}{\partial t} + \frac{1}{2} \left(\frac{\partial \rho u_j \phi}{\partial x_j} + \rho u_j \frac{\partial \phi}{\partial x_j} \right). \quad (12)$$

Again, the divergence form is primary conservative *a priori*, that is, conservative without the aid of the continuity. The secondary conservation property of the skew-symmetric form is demonstrated as follows:

$$\phi (\text{Skew.})_\phi = \frac{\partial \rho \phi^2 / 2}{\partial t} + \frac{\partial \rho u_j \phi^2 / 2}{\partial x_j}. \quad (13)$$

It is now possible to clarify the identities of the existing quasi-skew-symmetric forms by Feiereisen et al. [10] and Blaisdell et al. [11], and Morinishi et al. [15], respectively:

$$(\text{qSkD.})_\phi \equiv \frac{\partial \rho \phi}{\partial t} + \frac{1}{2} \left(\frac{\partial \rho u_j \phi}{\partial x_j} + \rho u_j \frac{\partial \phi}{\partial x_j} + \phi \frac{\partial \rho u_j}{\partial x_j} \right), \quad (14)$$

$$(\text{qSkA.})_\phi \equiv \rho \frac{\partial \phi}{\partial t} + \frac{1}{2} \left(\frac{\partial \rho u_j \phi}{\partial x_j} + \rho u_j \frac{\partial \phi}{\partial x_j} - \phi \frac{\partial \rho u_j}{\partial x_j} \right). \quad (15)$$

From Eqs. (9)–(11), these forms are analytically equivalent to the divergence and advective forms, respectively, and are not secondary conservative without the aid of the continuity:

$$(\text{qSkD.})_\phi = (\text{Skew.})_\phi + \frac{1}{2}\phi (\text{Cont.}) = (\text{Div.})_\phi, \quad (16)$$

$$(\text{qSkA.})_\phi = (\text{Skew.})_\phi - \frac{1}{2}\phi (\text{Cont.}) = (\text{Adv.})_\phi. \quad (17)$$

Fortunately, the numerical stabilities of these forms are much better than those with the divergence and advective forms as long as the last terms in (14) and (15) are discretized in the same manner as that in the discrete continuity. This implies that the stabilities of the quasi-symmetric forms are supported by the discrete consistency with the continuity. Note that an alternative quasi-skew-symmetric form based on the divergence one was used in Blaisdell et al. [12] and Ducros et al. [13,14].

$$(qSkD'.)_\phi \equiv \frac{\partial \rho \phi}{\partial t} + \frac{1}{2} \left(\frac{\partial \rho u_j \phi}{\partial x_j} + u_j \frac{\partial \rho \phi}{\partial x_j} + \rho \phi \frac{\partial u_j}{\partial x_j} \right). \tag{18}$$

This form can be rewritten as

$$(qSkD'.)_\phi = \frac{1}{2} (Div.v.)_\phi + \frac{1}{2} \left(\rho \frac{\partial \phi}{\partial t} + u_j \frac{\partial \rho \phi}{\partial x_j} \right) + \frac{1}{2} \phi \left(\frac{\partial \rho}{\partial t} + \rho \frac{\partial u_j}{\partial x_j} \right) = (Div.v.)_\phi, \tag{19}$$

and has no direct relation with the skew-symmetric form through the continuity for compressible flow, although it recovers the skew-symmetric form at the incompressible limit.

3. Analytical requirements

The governing equations for compressible flow considered in this study are the continuity, momentum, and internal energy equations as well as the equation of state:

$$(Cont.) = 0, \tag{20}$$

$$(Conv.)_i + (Pres.)_i = \frac{\partial \tau_{ij}}{\partial x_j}, \tag{21}$$

$$(Conv.)_e + (PD.)_e = \tau_{ij} \frac{\partial u_i}{\partial x_j} - \frac{\partial q_j}{\partial x_j}, \tag{22}$$

$$\text{with } p = p(\rho, e), \quad \text{or } \rho = \rho(p, e), \quad \text{or } e = e(\rho, p), \tag{23}$$

where

$$\tau_{ij} = \mu \left(\frac{\partial u_i}{\partial x_j} + \frac{\partial u_j}{\partial x_i} \right) - \frac{2}{3} \mu \frac{\partial u_k}{\partial x_k} \delta_{ij}, \quad q_j = -\kappa \frac{\partial T}{\partial x_j}. \tag{24}$$

In these equations, p is pressure, $e = C_v T$ is internal energy, T is temperature, C_v is the specific heat at constant volume, τ_{ij} are the components of viscous stress, q_j are the components of heat flux, μ is viscosity, and κ is thermal conductivity. The power law dependence of viscosity $\mu/\mu_0 = (T/T_0)^{0.76}$ is supposed, where μ_0 and T_0 are reference viscosity and temperature, respectively. For the ideal gas flow, $p(\rho, e) = (\gamma - 1)\rho e$, $\rho(p, e) = p/((\gamma - 1)e)$, and $e(\rho, p) = p/((\gamma - 1)\rho)$. The specific heat $\gamma \equiv C_p/C_v$ is set to 1.4, where C_p is the specific heat at constant pressure. The Prandtl number $Pr \equiv C_p \mu/\kappa$ is set to 0.71.

In the above equations, inviscid terms are written symbolically. $(Cont.)$ is the left-hand side of the continuity and defined in (5). $(Conv.)_i$ is a generic form of convective term in the momentum equation and takes one of the following forms, that is, divergence, advective, or skew-symmetric forms:

$$(Div.v.)_i \equiv \frac{\partial \rho u_i}{\partial t} + \frac{\partial \rho u_j u_i}{\partial x_j}, \tag{25}$$

$$(Adv.)_i \equiv \rho \frac{\partial u_i}{\partial t} + \rho u_j \frac{\partial u_i}{\partial x_j}, \tag{26}$$

$$(Skew.)_i \equiv \sqrt{\rho} \frac{\partial \sqrt{\rho} u_i}{\partial t} + \frac{1}{2} \left(\frac{\partial \rho u_j u_i}{\partial x_j} + \rho u_j \frac{\partial u_i}{\partial x_j} \right). \tag{27}$$

$(Conv.)_e$ is a generic form of a convective term in the internal energy equation and takes one of the following forms:

$$(Div.v.)_e \equiv \frac{\partial \rho e}{\partial t} + \frac{\partial \rho u_j e}{\partial x_j}, \tag{28}$$

$$(Adv.)_e \equiv \rho \frac{\partial e}{\partial t} + \rho u_j \frac{\partial e}{\partial x_j}, \tag{29}$$

$$(Skew.)_e \equiv \sqrt{\rho} \frac{\partial \sqrt{\rho} e}{\partial t} + \frac{1}{2} \left(\frac{\partial \rho u_j e}{\partial x_j} + \rho u_j \frac{\partial e}{\partial x_j} \right). \tag{30}$$

$(Pres.)_i$ and $(PD.)_e$ are the pressure term in the momentum equation and the pressure-dilatation term in the internal energy equation, respectively:

$$(Pres.)_i \equiv \frac{\partial p}{\partial x_i}, \tag{31}$$

$$(PD.)_e \equiv p \frac{\partial u_i}{\partial x_i}. \tag{32}$$

The commutability and secondary conservation property of the convective terms for the momentum equation are demonstrated as follows:

$$(Div.)_i = (Adv.)_i + u_i (Cont.), \quad (33)$$

$$(Skew.)_i = \frac{1}{2}(Div.)_i + \frac{1}{2}(Adv.)_i = (Div.)_i - \frac{1}{2}u_i (Cont.) = (Adv.)_i + \frac{1}{2}u_i (Cont.), \quad (34)$$

$$u_\alpha (Skew.)_\alpha = \frac{\partial \rho u_\alpha^2 / 2}{\partial t} + \frac{\partial \rho u_j u_\alpha^2 / 2}{\partial x_j}, \quad (35)$$

where the summation rule is not taken for the subscript α in the last equation. In the same way, the commutability and secondary conservation property of the convective terms for the internal energy equation are demonstrated as follows:

$$(Div.)_e = (Adv.)_e + e (Cont.), \quad (36)$$

$$(Skew.)_e = \frac{1}{2}(Div.)_e + \frac{1}{2}(Adv.)_e = (Div.)_e - \frac{1}{2}e (Cont.) = (Adv.)_e + \frac{1}{2}e (Cont.), \quad (37)$$

$$e (Skew.)_e = \frac{\partial \rho e^2 / 2}{\partial t} + \frac{\partial \rho u_j e^2 / 2}{\partial x_j}. \quad (38)$$

The total energy is one of the important conserved variables and is preferred in compressible flow simulations with strong discontinuity, since the solutions are often represented in weak form. For unsteady compressible flow simulations at low-Mach number, on the other hand, one of the thermodynamic variables (internal energy, enthalpy, entropy, etc.) is rather preferred than the total energy [19]. In this case, the total energy should be conditionally conserved.

The equation of total energy, $E = u_i u_i / 2 + e$, is obtained by adding the kinetic and internal energy equations. The kinetic energy equation is u_i times the i -component of (21) with summation over i . The use of skew-symmetric form in the kinetic energy equation is convenient for the derivation of the total energy equation.

$$\{u_i (Skew.)_i + (Div.)_e\} + \{u_i (Pres.)_i + (PD.)_e\} = \left\{ u_i \left(\frac{\partial \tau_{ij}}{\partial x_j} \right) + \left(\tau_{ij} \frac{\partial u_i}{\partial x_j} \right) \right\} - \frac{\partial q_j}{\partial x_j}. \quad (39)$$

The convective term in the total energy equation is composed of

$$u_i (Skew.)_i + (Div.)_e = \frac{\partial \rho E}{\partial t} + \frac{\partial \rho u_j E}{\partial x_j}. \quad (40)$$

This relation is useful for the specification of conserved discrete total energy norm. The pressure diffusion term in the total energy equation is composed of the pressure work term in the kinetic energy equation and the pressure-dilatation term in the internal energy equation.

$$u_i (Pres.)_i + (PD.)_e = \frac{\partial u_i p}{\partial x_i}. \quad (41)$$

In addition, the viscous diffusion term in the total energy equation is composed of the viscous stress work term in the kinetic energy equation and the viscous heating term in the internal energy equation.

$$u_i \left(\frac{\partial \tau_{ij}}{\partial x_j} \right) + \left(\tau_{ij} \frac{\partial u_i}{\partial x_j} \right) = \frac{\partial u_i \tau_{ij}}{\partial x_j}. \quad (42)$$

Therefore, the sum of these terms is conservative in the total energy equation.

The enthalpy, $h \equiv e + p/\rho$, is sometimes selected as an energy variable [18]. Its transport equation and accompanying state equation are as follows:

$$(Conv.)_h - (DpDt.)_h = \tau_{ij} \frac{\partial u_i}{\partial x_j} - \frac{\partial q_j}{\partial x_j}, \quad (43)$$

$$\text{with } p = p(\rho, h), \quad \text{or } \rho = \rho(p, h), \quad \text{or } h = h(\rho, p). \quad (44)$$

For the ideal gas flow, $p(\rho, h) = (\gamma - 1)\rho h/\gamma$, $\rho(p, h) = \gamma p/((\gamma - 1)h)$, and $h(\rho, p) = \gamma p/((\gamma - 1)\rho)$. The total energy is composed of $E = u_i u_i / 2 + h - p/\rho$ with enthalpy. $(Conv.)_h$ is a generic form of convective term in the enthalpy equation and takes the same form of convective term for $(Conv.)_e$, where e is replaced by h . $(DpDt.)_h$ is the material derivative of pressure in the enthalpy equation defined by

$$(DpDt.)_h \equiv \frac{\partial p}{\partial t} + u_i \frac{\partial p}{\partial x_i}. \quad (45)$$

The equation of total energy is also derived by adding the kinetic energy and enthalpy equations:

$$\{u_i (Skew.)_i + (Div.)_h\} + \{u_i (Pres.)_i - (DpDt.)_h\} = \left\{ u_i \left(\frac{\partial \tau_{ij}}{\partial x_j} \right) + \left(\tau_{ij} \frac{\partial u_i}{\partial x_j} \right) \right\} - \frac{\partial q_j}{\partial x_j}. \quad (46)$$

The left-hand side of the above equation is rewritten in the conservative form as

$$\{u_i (Skew.)_i + (Div.)_h\} + \{u_i (Pres.)_i - (DpDt.)_h\} = \frac{\partial \rho E}{\partial t} + \frac{\partial \rho u_j H}{\partial x_j}, \tag{47}$$

where $H = u_i u_i / 2 + h$ is the total enthalpy.

The objective of this work is to derive the fully conservative finite difference schemes for compressible flow that satisfy these properties in a discrete sense.

4. Fully discrete finite difference schemes

In this and the following sections, analysis is limited to a uniform staggered grid system for clarity and suitability at a low-Mach number. The internal energy is chosen as an energy variable. For the reader’s convenience, schemes in a regular grid system are given in Appendix A, and fully conservative schemes in a non-uniform staggered grid system are presented in Appendix B. The scheme in a non-uniform staggered grid system with enthalpy as an energy variable is included in Appendix B.

4.1. Discrete operators

In this study, spatio-temporal discrete values are represented as $\phi_{i,j,k}^n \equiv \phi((x_1)_i, (x_2)_j, (x_3)_k; (t)^n)$, where $(x_1)_i = i\Delta x_1$, $(x_2)_j = j\Delta x_2$, $(x_3)_k = k\Delta x_3$, and $(t)^n = n\Delta t$. The grid spacings, Δx_1 , Δx_2 , and Δx_3 , are constant, and Δt is the time increment. Mid-points are denoted like $i + 1/2$.

Finite difference, interpolation and permanent product in x_1 direction with stencil width m are defined, respectively, as [1]

$$\frac{\delta_m \phi}{\delta_m x_1} \Big|_{i,j,k} \equiv \frac{\phi_{i+m/2,j,k} - \phi_{i-m/2,j,k}}{m\Delta x_1}, \tag{48}$$

$$\overline{\phi}^{-mx_1} \Big|_{i,j,k} \equiv \frac{\phi_{i+m/2,j,k} + \phi_{i-m/2,j,k}}{2}, \tag{49}$$

$$\widetilde{\phi \psi}^{mx_1} \Big|_{i,j,k} \equiv \frac{\phi_{i+m/2,j,k} \psi_{i-m/2,j,k} + \psi_{i+m/2,j,k} \phi_{i-m/2,j,k}}{2}. \tag{50}$$

Discrete operators in x_2 and x_3 directions are defined in the same way as for x_1 direction. The index j in the finite difference $\delta_m \phi / \delta_m x_j$ is physical and follows the summation convention. On the other hand, the indices j in $\overline{\phi}^{-mx_j}$ and $\widetilde{\phi \psi}^{mx_j}$ are numerical and do not follow the convention. These numerical indices take the same value as the same physical index in the same term. Finite difference and interpolation in time with stencil width 1 are also defined as [16]

$$\frac{\delta_1 \phi}{\delta_1 t} \Big|^{n+1/2} = \frac{\phi^{n+1} - \phi^n}{\Delta t}, \tag{51}$$

$$\overline{\phi}^{-1t} \Big|^{n+1/2} = \frac{\phi^{n+1} + \phi^n}{2}. \tag{52}$$

The following identities [1] will be used to derive some relations later in this study:

$$\frac{\delta_m \overline{\phi}^{-lx_i}}{\delta_m x_j} = \frac{\delta_m \overline{\phi}^{-lx_i}}{\delta_m x_j}, \tag{53}$$

$$\frac{\delta_{2m} \phi}{\delta_{2m} x_j} = \frac{\delta_m \overline{\phi}^{-mx_j}}{\delta_m x_j}, \tag{54}$$

$$\psi \frac{\delta_{2m} \phi}{\delta_{2m} x_j} + \phi \frac{\delta_{2m} \psi}{\delta_{2m} x_j} = \frac{\delta_m \widetilde{\psi \phi}^{mx_j}}{\delta_m x_j}, \tag{55}$$

$$\overline{\psi} \frac{\delta_m \phi}{\delta_m x_j} + \phi \frac{\delta_m \psi}{\delta_m x_j} = \frac{\delta_m \overline{\psi \phi}^{-mx_j}}{\delta_m x_j}, \tag{56}$$

$$\phi \left(\frac{\delta_m \psi \overline{\phi}^{-mx_j}}{\delta_m x_j} + \psi \frac{\delta_m \overline{\phi}^{-mx_j}}{\delta_m x_j} \right) = \frac{\delta_m \widetilde{\psi \phi}^{mx_j}}{\delta_m x_j}, \tag{57}$$

$$\frac{\delta_1 \overline{\phi}^{-1t}}{\delta_1 t} = \frac{\delta_1 \overline{\phi}^{-1t}}{\delta_1 t}, \tag{58}$$

$$\overline{\psi} \frac{\delta_1 \phi}{\delta_1 t} + \overline{\phi}^{-1t} \frac{\delta_1 \psi}{\delta_1 t} = \frac{\delta_1 \overline{\psi \phi}^{-1t}}{\delta_1 t}, \tag{59}$$

$$\overline{\phi}^{-1t} \frac{\delta_1 \phi}{\delta_1 t} = \frac{1}{2} \frac{\delta_1 \phi^2}{\delta_1 t}, \quad \sqrt{\overline{\phi}^{-1t}} \frac{\delta_1 \sqrt{\phi}}{\delta_1 t} = \frac{1}{2} \frac{\delta_1 \phi}{\delta_1 t}, \tag{60}$$

$$\overline{\overline{\phi}^{-1t}}^{mx_i} = \overline{\overline{\phi}^{-1t}}^{mx_i}, \quad \frac{\delta_1 \overline{\phi}^{-1t}}{\delta_1 t} = \frac{\delta_1 \overline{\phi}^{-1t}}{\delta_1 t}, \quad \frac{\delta_m \overline{\phi}^{-1t}}{\delta_m x_j} = \frac{\delta_m \overline{\phi}^{-1t}}{\delta_m x_j}. \tag{61}$$

4.2. Fully conservative second-order accurate finite difference scheme in a staggered grid system

In this subsection, a finite difference scheme in a spatio-temporal staggered grid system like Pierce et al. [17] and Wall et al. [18] is discussed. An example of the staggered grid system on $x_1 - x_2$ plane is shown in Fig. 1(a). Each velocity component is staggered in space by one-half grid spacing with respect to the scalar variables [2]. Fig. 1(b) shows an example of the staggered grid system on $x_1 - t$ plane. The main difference from the spatio-temporal grid system by Pierce et al. [17] and Wall et al. [18] is the temporal arrangement of internal energy. The energy variable is arranged at the same temporal level as that for the velocity. This arrangement makes the definition of discrete total energy norm unambiguous as shown later (in (83) and (84)). In addition, the diagonal components of stress tensor are defined at the center of cells, while the off-diagonal components are defined on different edges.

Based on the analytical requirements of the governing equations and the relation between discrete operators, we can construct fully discrete fully conservative second-order accurate finite difference scheme for (20)–(23):

$$(Cont.-FS2) = 0, \tag{62}$$

$$(Conv.-FS2)_i + (Pres.-FS2)_i = \frac{\delta_1 \tau_{ij}}{\delta_1 x_j}, \tag{63}$$

$$(Conv.-FS2)_e + (PD.-FS2)_e = \left(\tau_{ij} \odot \frac{\delta_1 \hat{u}_i}{\delta_1 x_j} \right) - \frac{\delta_1 q_j}{\delta_1 x_j}, \tag{64}$$

$$\text{with } \bar{\rho}^{1t} = p(\bar{\rho}^{1t}, e), \text{ or } \bar{\rho}^{1t} = \rho(\bar{p}^{1t}, e), \text{ or } e = e(\bar{\rho}^{1t}, \bar{p}^{1t}). \tag{65}$$

\hat{u}_i is a special interpolation of the velocity and defined later in (74). In this study, discretizations are done at possible spatio-temporal locations corresponding to the discrete operators and the configuration of discrete variables. For instance, the discrete continuity is defined at the point of internal energy. Inviscid terms are denoted symbolically, where $-FS2$ denotes a fully discrete second-order accurate approximation in a staggered grid system. $(Cont.-FS2)$ is the left-hand side of the continuity.

$$(Cont.-FS2) \equiv \frac{\delta_1 \rho}{\delta_1 t} + \frac{\delta_1 g_j}{\delta_1 x_j} (= 0), \tag{66}$$

where g_j is the numerical mass flux for the second-order scheme in a staggered grid system defined by

$$g_j \equiv \overline{\overline{\rho}^{1t}}^{1x_j} u_j. \tag{67}$$

$(Conv.-FS2)_i$ is a generic form of the convection scheme for the momentum equation and takes one of the following three forms, that is, divergence, advective and skew-symmetric forms:

$$(Div.-FS2)_i \equiv \frac{\delta_1 \overline{\overline{\rho}^{1t}}^{1x_i} u_i}{\delta_1 t} + \frac{\delta_1 \overline{\overline{g}_j^{1t}}^{1x_j} \overline{\overline{u}_i}^{1x_j}}{\delta_1 x_j}, \tag{68}$$

$$(Adv.-FS2)_i \equiv \overline{\overline{\rho}^{1t}}^{1x_i} \frac{\delta_1 u_i}{\delta_1 t} + \left(\overline{\overline{u}_i}^{1t} - \hat{u}_i \right) \frac{\delta_1 \overline{\overline{\rho}^{1t}}^{1x_i}}{\delta_1 t} + \overline{\overline{g}_j^{1t}}^{1x_j} \frac{\delta_1 \overline{\overline{u}_i}^{1x_j}}{\delta_1 x_j}, \tag{69}$$

$$(Skew.-FS2)_i \equiv \sqrt{\overline{\overline{\rho}^{1t}}^{1x_i}} \frac{\delta_1 \sqrt{\overline{\overline{\rho}^{1t}}^{1x_i}} u_i}{\delta_1 t} + \frac{1}{2} \left(\frac{\delta_1 \overline{\overline{g}_j^{1t}}^{1x_j} \overline{\overline{u}_i}^{1x_j}}{\delta_1 x_j} + \overline{\overline{g}_j^{1t}}^{1x_j} \frac{\delta_1 \overline{\overline{u}_i}^{1x_j}}{\delta_1 x_j} \right), \tag{70}$$

where the second term in the right-hand side of $(Adv.-FS2)_i$ is required for the commutability with $(Div.-FS2)_i$ and $(Skew.-FS2)_i$, although it seems to be anomalous. $(Conv.-FS2)_e$ is a generic form of the convection scheme for the internal energy equation and takes one of the following forms:

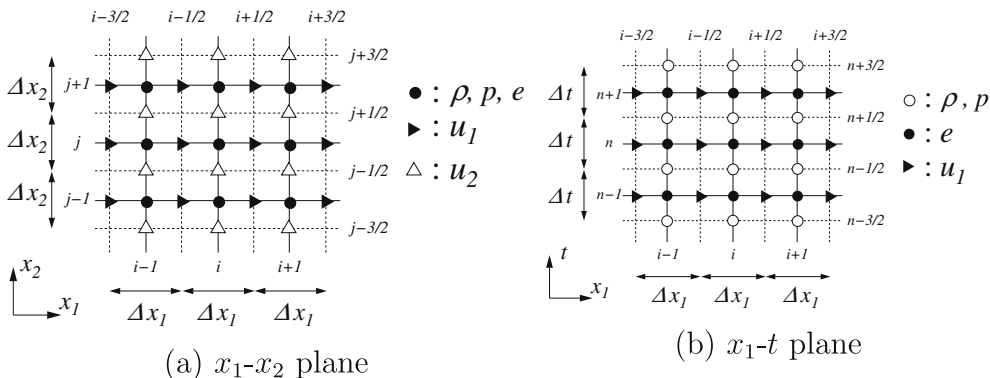


Fig. 1. Spatio-temporal staggered grid system. $i, j,$ and n are spatio-temporal location indices.

$$(Div.-FS2)_e \equiv \frac{\delta_1 \bar{\rho}^{1t} e}{\delta_1 t} + \frac{\delta_1 \bar{g}_j^{-1t} \bar{e}^{-1x_j}}{\delta_1 x_j}, \tag{71}$$

$$(Adv.-FS2)_e \equiv \bar{\rho}^{1t} \frac{\delta_1 e}{\delta_1 t} + (\bar{e}^{1t} - \hat{e}) \frac{\delta_1 \bar{\rho}^{1t}}{\delta_1 t} + \bar{g}_j^{-1t} \frac{\delta_1 \bar{e}^{-1x_j}}{\delta_1 x_j}, \tag{72}$$

$$(Skew.-FS2)_e \equiv \sqrt{\bar{\rho}^{1t}} \frac{\delta_1 \sqrt{\bar{\rho}^{1t}} e}{\delta_1 t} + \frac{1}{2} \left(\frac{\delta_1 \bar{g}_j^{-1t} \bar{e}^{-1x_j}}{\delta_1 x_j} + \frac{\delta_1 \bar{e}^{-1x_j}}{\delta_1 x_j} \right). \tag{73}$$

\hat{u}_i and \hat{e} are special interpolations which require for the construction of fully discrete fully conservative schemes:

$$\hat{u}_i \equiv \frac{\sqrt{\bar{\rho}^{1t} u_i}}{\sqrt{\bar{\rho}^{1t}}}, \quad \hat{e} \equiv \frac{\sqrt{\bar{\rho}^{1t}} e}{\sqrt{\bar{\rho}^{1t}}}. \tag{74}$$

The square-root density weighted interpolation was independently derived by Morinishi [20] and Subbareddy and Candler [21]. The derivation by Subbareddy and Candler [21] is based on the Roe’s parameter vector [22]. The author’s derivation [20] is more straightforward and based on the discrete form of the temporal derivative term in the skew-symmetric form. For instance, \hat{e} is derived so as to satisfy the following relation:

$$\hat{e} \left(\sqrt{\bar{\rho}^{1t}} \frac{\delta_1 \sqrt{\bar{\rho}^{1t}} e}{\delta_1 t} \right) = \frac{\delta_1 \bar{\rho}^{1t} e^2 / 2}{\delta_1 t}.$$

The term in parentheses is a natural discrete form for the temporal derivative term in (30) and shown in (73). The right-hand side of the above equation is rewritten using (60) as

$$\frac{\delta_1 \bar{\rho}^{1t} e^2 / 2}{\delta_1 t} = \sqrt{\bar{\rho}^{1t}} e \frac{\delta_1 \sqrt{\bar{\rho}^{1t}} e}{\delta_1 t} = \left(\frac{\sqrt{\bar{\rho}^{1t}} e}{\sqrt{\bar{\rho}^{1t}}} \right) \left(\sqrt{\bar{\rho}^{1t}} \frac{\delta_1 \sqrt{\bar{\rho}^{1t}} e}{\delta_1 t} \right).$$

Comparing these equations, the definition of \hat{e} in (74) is obtained. Then, the spatial derivative term in the skew-symmetric form of (73) is derived to satisfy the secondary conservation property using (57) and \hat{e} .

$(Pres.-FS2)_i$ and $(PD.-FS2)_e$ are the discrete pressure term in the momentum equation and the discrete pressure-dilatation term in the internal energy equation defined, respectively, by

$$(Pres.-FS2)_i \equiv \frac{\delta_1 \bar{p}^{1t}}{\delta_1 x_i}, \tag{75}$$

$$(PD.-FS2)_e \equiv \bar{p}^{1t} \frac{\delta_1 \hat{u}_i}{\delta_1 x_i}. \tag{76}$$

The double temporal interpolation on the pressure was introduced by Wall et al. [18] to make the pressure term implicit.

Discrete commutability between the divergence and advective forms for the momentum equation is demonstrated using (53), (56), (58), (59) and (61) as follows:

$$(Div.-FS2)_i = (Adv.-FS2)_i + \hat{u}_i \frac{\delta_1 \bar{p}^{1t}}{\delta_1 x_i}. \tag{77}$$

The relation for the skew-symmetric form for the momentum equation is demonstrated using (59), (60) and (77) as

$$\begin{aligned} (Skew.-FS2)_i &= \frac{1}{2} (Div.-FS2)_i + \frac{1}{2} (Adv.-FS2)_i = (Div.-FS2)_i - \frac{1}{2} \hat{u}_i \frac{\delta_1 \bar{p}^{1t}}{\delta_1 x_i} \\ &= (Adv.-FS2)_i + \frac{1}{2} \hat{u}_i \frac{\delta_1 \bar{p}^{1t}}{\delta_1 x_i}. \end{aligned} \tag{78}$$

The secondary conservation property of the skew-symmetric form for the momentum equation is also demonstrated using (57) and (60) as

$$\hat{u}_\alpha (Skew.-FS2)_\alpha = \frac{\delta_1 \bar{\rho}^{1x_\alpha} u_\alpha^2 / 2}{\delta_1 t} + \frac{\delta_1 \bar{g}_j^{-1x_\alpha} \hat{u}_\alpha \hat{u}_\alpha^{1x_j} / 2}{\delta_1 x_j}, \tag{79}$$

where the summation rule is not taken for the subscript α . These are discrete analogues of (33)–(35). The commutability and secondary conservation property of the convection schemes for the internal energy equation are also demonstrated in the same way:

$$(Div.-FS2)_e = (Adv.-FS2)_e + \hat{e} \overline{(Cont.-FS2)}^{1t}, \tag{80}$$

$$(Skew.-FS2)_e = \frac{1}{2}(Div.-FS2)_e + \frac{1}{2}(Adv.-FS2)_e = (Div.-FS2)_e - \frac{1}{2}\hat{e} \overline{(Cont.-FS2)}^{1t} = (Adv.-FS2)_e + \frac{1}{2}\hat{e} \overline{(Cont.-FS2)}^{1t}, \tag{81}$$

$$\hat{e} (Skew.-FS2)_e = \frac{\delta_1 \bar{\rho}^{1t} e^2 / 2}{\delta_1 t} + \frac{\delta_1 \bar{g}_j^{1t} \hat{e} \tilde{e}^{1x_j} / 2}{\delta_1 x_j}. \tag{82}$$

The convective term of the total energy equation obtained as a result is written as the following form using (53), (57) and (60),

$$\widehat{u}_i (Skew.-FS2)_i^{1x_i} + (Div.-FS2)_e = \frac{\delta_1 (\rho E)_{FS2}}{\delta_1 t} + \frac{\delta_1}{\delta_1 x_j} \left(\frac{1}{2} \overline{\bar{g}_j^{1t} \widehat{u}_i \tilde{e}^{1x_j}}^{1x_i} + \bar{g}_j^{1t} \bar{e}^{1x_j} \right), \tag{83}$$

where $(\rho E)_{FS2}$ is the discrete total energy norm conserved by the second-order scheme;

$$(\rho E)_{FS2} \equiv \frac{1}{2} \overline{\bar{\rho}^{1t} u_i u_i}^{1x_i} + \bar{\rho}^{1t} e. \tag{84}$$

The conservation property of the pressure term in the total energy equation is then demonstrated using (56) as

$$\widehat{u}_i (Pres.-FS2)_i^{1x_i} + (PD.-FS2)_e = \frac{\delta_1 \widehat{u}_i \overline{\bar{\rho}^{1t}}^{1x_i}}{\delta_1 x_i}. \tag{85}$$

The total energy conservation for the viscous term is also demonstrated as follows:

$$\widehat{u}_i \frac{\delta_1 \tau_{ij}}{\delta_1 x_j}^{1x_i} + \left(\tau_{ij} \odot \frac{\delta_1 \widehat{u}_i}{\delta_1 x_j} \right) = \left(\frac{\delta_1 \widehat{u}_i \odot \tau_{ij}}{\delta_1 x_j} \right), \tag{86}$$

where

$$\begin{aligned} \left(\tau_{ij} \odot \frac{\delta_1 \widehat{u}_i}{\delta_1 x_j} \right) &\equiv \left(\tau_{11} \frac{\delta_1 \widehat{u}_1}{\delta_1 x_1} + \tau_{22} \frac{\delta_1 \widehat{u}_2}{\delta_1 x_2} + \tau_{33} \frac{\delta_1 \widehat{u}_3}{\delta_1 x_3} \right) + \tau_{12} \left(\frac{\delta_1 \widehat{u}_1}{\delta_1 x_2} + \frac{\delta_1 \widehat{u}_2}{\delta_1 x_1} \right) + \tau_{13} \left(\frac{\delta_1 \widehat{u}_1}{\delta_1 x_3} + \frac{\delta_1 \widehat{u}_3}{\delta_1 x_1} \right) \\ &\quad + \tau_{23} \left(\frac{\delta_1 \widehat{u}_2}{\delta_1 x_3} + \frac{\delta_1 \widehat{u}_3}{\delta_1 x_2} \right) \end{aligned} \tag{87}$$

is the discrete viscous heating term in the internal energy equation, and

$$\begin{aligned} \left(\frac{\delta_1 \widehat{u}_i \odot \tau_{ij}}{\delta_1 x_j} \right) &\equiv \frac{\delta_1 \left(\widehat{u}_1 \overline{\tau_{11}}^{1x_1} + \widehat{u}_2 \overline{\tau_{21}}^{1x_2} + \widehat{u}_3 \overline{\tau_{32}}^{1x_3} \right)}{\delta_1 x_1} + \frac{\delta_1 \left(\widehat{u}_1 \overline{\tau_{21}}^{1x_2} + \widehat{u}_2 \overline{\tau_{11}}^{1x_2} + \widehat{u}_3 \overline{\tau_{32}}^{1x_3} \right)}{\delta_1 x_2} \\ &\quad + \frac{\delta_1 \left(\widehat{u}_1 \overline{\tau_{31}}^{1x_3} + \widehat{u}_2 \overline{\tau_{32}}^{1x_3} + \widehat{u}_3 \overline{\tau_{33}}^{1x_3} \right)}{\delta_1 x_3} \end{aligned} \tag{88}$$

is the viscous diffusion term in the discrete total energy equation.

The present fully discrete scheme is fully conservative at the inviscid limit in the following sense: the convection schemes for divergence and skew-symmetric forms are primary and secondary conservative, respectively, without the aid of the discrete continuity; the convection schemes for divergence, advective, and skew-symmetric forms are commutable if the discrete continuity is satisfied; and the sum of the pressure work term in the consequent kinetic energy equation and the pressure-dilatation term in the internal energy equation is conservative. These constraints are exactly satisfied in the spatio-temporal discretization. In the present scheme, the sum of the viscous work term in the kinetic energy equation and the viscous heating term in the internal energy equation is also conservative, although this condition is not mandatory for stable unsteady simulation at high Reynolds number. In addition, the present discretization for the continuity and momentum equations reduces to the fully discrete fully conservative scheme for incompressible flow by Ham et al. [16] at the limit of constant density.

4.3. Spatially fourth-order accurate fully conservative finite difference scheme in a staggered grid system

In this subsection, spatially fourth-order fully discrete fully conservative schemes for the inviscid terms are constructed based on the same way as in Morinishi et al. [1]. Commutability and secondary conservation property of the convection schemes and the energy conservation property of the pressure-related terms are demonstrated in the same way as those for the second-order scheme. Therefore, the corresponding discrete properties are presented without any proofs. The scheme for the left-hand side of the continuity is

$$(Cont.-FS4_2) \equiv \frac{\delta_1 \rho}{\delta_1 t} + \left(\frac{9}{8} \frac{\delta_1 g_j}{\delta_1 x_j} - \frac{1}{8} \frac{\delta_3 g_j}{\delta_3 x_j} \right) (= 0), \tag{89}$$

where $-FS4_2$ denotes a fully discrete spatially fourth-order accurate approximation in a staggered grid system with the second-order accurate temporal discretization. In this subsection, the numerical mass flux is replaced by

$$g_j \equiv \overline{\overline{\overline{\overline{\rho}}^{1t}}^{4thx_j}} u_j, \tag{90}$$

where $\overline{\overline{\overline{\overline{\phi}}^{4thx_j}} \equiv (9\overline{\overline{\overline{\overline{\phi}}^{1x_j}} - \overline{\overline{\overline{\overline{\phi}}^{3x_j}}})/8$ is the fourth-order accurate spatial interpolation. The fourth-order accurate convection schemes for the momentum equation with the divergence, advective, and skew-symmetric forms are defined, respectively, as

$$(Div.-FS4_2)_i \equiv \frac{\delta_1 \overline{\overline{\overline{\overline{\rho}}^{1t}}^{4thx_i}} u_i}{\delta_1 t} + \left(\frac{9}{8} \frac{\delta_1 \overline{\overline{\overline{\overline{g}}^{1t}}^{4thx_i}} \overline{\overline{\overline{\overline{u}}^{1x_i}}}}{\delta_1 x_j} - \frac{1}{8} \frac{\delta_3 \overline{\overline{\overline{\overline{g}}^{1t}}^{4thx_i}} \overline{\overline{\overline{\overline{u}}^{3x_i}}}}{\delta_3 x_j} \right), \tag{91}$$

$$(Adv.-FS4_2)_i \equiv \overline{\overline{\overline{\overline{\rho}}^{1t}}^{4thx_i}} \frac{\delta_1 u_i}{\delta_1 t} + (\overline{\overline{\overline{\overline{u}}^{1t}} - \widehat{u}_i) \frac{\delta_1 \overline{\overline{\overline{\overline{\rho}}^{1t}}^{4thx_i}}}{\delta_1 t} + \left(\frac{9}{8} \frac{\overline{\overline{\overline{\overline{g}}^{1t}}^{4thx_i}} \delta_1 \overline{\overline{\overline{\overline{u}}^{1x_i}}}}{\delta_1 x_j} - \frac{1}{8} \frac{\overline{\overline{\overline{\overline{g}}^{1t}}^{4thx_i}} \delta_3 \overline{\overline{\overline{\overline{u}}^{3x_i}}}}{\delta_3 x_j} \right), \tag{92}$$

$$(Skew.-FS4_2)_i \equiv \sqrt{\overline{\overline{\overline{\overline{\rho}}^{1t}}^{4thx_i}}} \frac{\delta_1 \sqrt{\overline{\overline{\overline{\overline{\rho}}^{1t}}^{4thx_i}}} u_i}{\delta_1 t} + \frac{1}{2} \left(\frac{9}{8} \frac{\delta_1 \overline{\overline{\overline{\overline{g}}^{1t}}^{4thx_i}} \overline{\overline{\overline{\overline{u}}^{1x_j}}}}{\delta_1 x_j} - \frac{1}{8} \frac{\delta_3 \overline{\overline{\overline{\overline{g}}^{1t}}^{4thx_i}} \overline{\overline{\overline{\overline{u}}^{3x_j}}}}{\delta_3 x_j} \right) + \frac{1}{2} \left(\frac{9}{8} \frac{\overline{\overline{\overline{\overline{g}}^{1t}}^{4thx_i}} \delta_1 \overline{\overline{\overline{\overline{u}}^{1x_j}}}}{\delta_1 x_j} - \frac{1}{8} \frac{\overline{\overline{\overline{\overline{g}}^{1t}}^{4thx_i}} \delta_3 \overline{\overline{\overline{\overline{u}}^{3x_j}}}}{\delta_3 x_j} \right), \tag{93}$$

where the square-root density weighted interpolation of velocity is replaced by

$$\widehat{u}_i \equiv \frac{\sqrt{\overline{\overline{\overline{\overline{\rho}}^{1t}}^{4thx_i}}} u_i}{\sqrt{\overline{\overline{\overline{\overline{\rho}}^{1t}}^{4thx_i}}}. \tag{94}$$

The fourth-order accurate convection schemes for the internal energy equation are also defined in the same manner as follows:

$$(Div.-FS4_2)_e \equiv \frac{\delta_1 \overline{\overline{\overline{\overline{\rho}}^{1t}} e}}{\delta_1 t} + \left(\frac{9}{8} \frac{\delta_1 \overline{\overline{\overline{\overline{g}}^{1t}} e^{-1x_j}}}{\delta_1 x_j} - \frac{1}{8} \frac{\delta_3 \overline{\overline{\overline{\overline{g}}^{1t}} e^{-3x_j}}}{\delta_3 x_j} \right), \tag{95}$$

$$(Adv.-FS4_2)_e \equiv \overline{\overline{\overline{\overline{\rho}}^{1t}} e} \frac{\delta_1 e}{\delta_1 t} + (\overline{\overline{\overline{\overline{e}}^{1t}} - \widehat{e}) \frac{\delta_1 \overline{\overline{\overline{\overline{\rho}}^{1t}}}}{\delta_1 t} + \left(\frac{9}{8} \frac{\overline{\overline{\overline{\overline{g}}^{1t}} \delta_1 \widehat{e}^{-1x_j}}}{\delta_1 x_j} - \frac{1}{8} \frac{\overline{\overline{\overline{\overline{g}}^{1t}} \delta_3 \widehat{e}^{-3x_j}}}{\delta_3 x_j} \right), \tag{96}$$

$$(Skew.-FS4_2)_e \equiv \sqrt{\overline{\overline{\overline{\overline{\rho}}^{1t}}}} \frac{\delta_1 \sqrt{\overline{\overline{\overline{\overline{\rho}}^{1t}}}} e}{\delta_1 t} + \frac{1}{2} \left(\frac{9}{8} \frac{\delta_1 \overline{\overline{\overline{\overline{g}}^{1t}} e^{-1x_j}}}{\delta_1 x_j} - \frac{1}{8} \frac{\delta_3 \overline{\overline{\overline{\overline{g}}^{1t}} e^{-3x_j}}}{\delta_3 x_j} \right) + \frac{1}{2} \left(\frac{9}{8} \frac{\overline{\overline{\overline{\overline{g}}^{1t}} \delta_1 \widehat{e}^{-1x_j}}}{\delta_1 x_j} - \frac{1}{8} \frac{\overline{\overline{\overline{\overline{g}}^{1t}} \delta_3 \widehat{e}^{-3x_j}}}{\delta_3 x_j} \right). \tag{97}$$

The square-root density weighted interpolation of internal energy, \widehat{e} , is the same as that for the second-order scheme as shown in (74). The fourth-order discrete forms for the pressure-related terms in the momentum and internal equations are

$$(Pres.-FS4_2)_i \equiv \frac{9}{8} \frac{\delta_1 \overline{\overline{\overline{\overline{\rho}}^{1t}}}}{\delta_1 x_i} - \frac{1}{8} \frac{\delta_3 \overline{\overline{\overline{\overline{\rho}}^{1t}}}}{\delta_3 x_i}, \tag{98}$$

$$(PD.-FS4_2)_e \equiv \overline{\overline{\overline{\overline{\rho}}^{1t}}} \left(\frac{9}{8} \frac{\delta_1 \widehat{u}_i}{\delta_1 x_i} - \frac{1}{8} \frac{\delta_3 \widehat{u}_i}{\delta_3 x_i} \right). \tag{99}$$

Commutability and secondary conservation property of the convection schemes for the momentum equation are demonstrated as follows:

$$(Div.-FS4_2)_i = (Adv.-FS4_2)_i + \widehat{u}_i \left\{ \frac{9}{8} \frac{\overline{\overline{\overline{\overline{\rho}}^{1t}}^{1x_i}}}{(Cont.-FS4_2)} - \frac{1}{8} \frac{\overline{\overline{\overline{\overline{\rho}}^{1t}}^{3x_i}}}{(Cont.-FS4_2)} \right\}, \tag{100}$$

$$(Skew.-FS4_2)_i = \frac{1}{2} (Div.-FS4_2)_i + \frac{1}{2} (Adv.-FS4_2)_i = (Div.-FS4_2)_i - \frac{1}{2} \widehat{u}_i \left\{ \frac{9}{8} \frac{\overline{\overline{\overline{\overline{\rho}}^{1t}}^{1x_i}}}{(Cont.-FS4_2)} - \frac{1}{8} \frac{\overline{\overline{\overline{\overline{\rho}}^{1t}}^{3x_i}}}{(Cont.-FS4_2)} \right\} = (Adv.-FS4_2)_i + \frac{1}{2} \widehat{u}_i \left\{ \frac{9}{8} \frac{\overline{\overline{\overline{\overline{\rho}}^{1t}}^{1x_i}}}{(Cont.-FS4_2)} - \frac{1}{8} \frac{\overline{\overline{\overline{\overline{\rho}}^{1t}}^{3x_i}}}{(Cont.-FS4_2)} \right\}, \tag{101}$$

$$\widehat{u}_\alpha (Skew.-FS4_2)_\alpha = \frac{\delta_1 \overline{\overline{\overline{\overline{\rho}}}}^{4thx_\alpha} u_\alpha^2 / 2}{\delta_1 t} + \frac{9}{8} \frac{\delta_1 \overline{\overline{\overline{\overline{g}}}}^{4thx_\alpha} \widehat{u}_\alpha \widehat{u}_\alpha^{1x_j} / 2}{\delta_1 x_j} - \frac{1}{8} \frac{\delta_3 \overline{\overline{\overline{\overline{g}}}}^{4thx_\alpha} \widehat{u}_\alpha \widehat{u}_\alpha^{3x_j} / 2}{\delta_3 x_j}, \tag{102}$$

where the summation rule is not taken for the subscript α in the last equation. The commutability and secondary conservation property of the convection schemes for the internal energy equation are also indicated as follows:

$$(Div.-FS4_2)_e = (Adv.-FS4_2)_e + \widehat{e} (\overline{Cont.-FS4})^{1t}, \tag{103}$$

$$(Skew.-FS4_2)_e = \frac{1}{2} (Div.-FS4_2)_e + \frac{1}{2} (Adv.-FS4_2)_e = (Div.-FS4_2)_e - \frac{1}{2} \widehat{e} (\overline{Cont.-FS4})^{1t} = (Adv.-FS4_2)_e + \frac{1}{2} \widehat{e} (\overline{Cont.-FS4})^{1t}, \tag{104}$$

$$\widehat{e} (Skew.-FS4_2)_e = \frac{\delta_1 \overline{\overline{\overline{\overline{\rho}}}}^{1t} e^2 / 2}{\delta_1 t} + \frac{9}{8} \frac{\delta_1 \overline{\overline{\overline{\overline{g}}}}^{1t} \widehat{e} \widehat{e}^{1x_j} / 2}{\delta_1 x_j} - \frac{1}{8} \frac{\delta_3 \overline{\overline{\overline{\overline{g}}}}^{1t} \widehat{e} \widehat{e}^{3x_j} / 2}{\delta_3 x_j}. \tag{105}$$

The convective term of the total energy equation obtained as a result is written in the following form:

$$\left\{ \frac{9}{8} \overline{\overline{\overline{\overline{\widehat{u}}}}}_i^{1x_i} (Skew.-FS4_2)_i - \frac{1}{8} \overline{\overline{\overline{\overline{\widehat{u}}}}}_i^{3x_i} (Skew.-FS4_2)_i \right\} + (Div.-FS4_2)_e = \frac{\delta_1 (\rho E)_{FS4_2}}{\delta_1 t} + \frac{9}{8} \frac{\delta_1}{\delta_1 x_j} \left(\frac{1}{2} \overline{\overline{\overline{\overline{\widehat{u}}}}}_i^{4thx_i} \widehat{u}_i \widehat{u}_i^{1x_j} + \overline{\overline{\overline{\overline{\widehat{u}}}}}_i^{1x_j} \right) - \frac{1}{8} \frac{\delta_3}{\delta_3 x_j} \left(\frac{1}{2} \overline{\overline{\overline{\overline{\widehat{u}}}}}_i^{4thx_i} \widehat{u}_i \widehat{u}_i^{3x_j} + \overline{\overline{\overline{\overline{\widehat{u}}}}}_i^{3x_j} \right), \tag{106}$$

where conserved discrete total energy norm for the fourth-order scheme, $(\rho E)_{FS4_2}$, is

$$(\rho E)_{FS4_2} \equiv \frac{1}{2} \overline{\overline{\overline{\overline{\rho}}}}^{4thx_i} u_i u_i + \overline{\overline{\overline{\overline{\rho}}}}^{1t} e. \tag{107}$$

The conservation property of the pressure term in the total energy equation is then demonstrated as

$$\left\{ \frac{9}{8} \overline{\overline{\overline{\overline{\widehat{u}}}}}_i^{1x_i} (Pres.-FS4_2)_i - \frac{1}{8} \overline{\overline{\overline{\overline{\widehat{u}}}}}_i^{3x_i} (Pres.-FS4_2)_i \right\} + (PD.-FS4_2)_e = \frac{9}{8} \frac{\delta_1 \widehat{u}_i \overline{\overline{\overline{\overline{\rho}}}}^{1t}^{1x_i}}{\delta_1 x_i} - \frac{1}{8} \frac{\delta_3 \widehat{u}_i \overline{\overline{\overline{\overline{\rho}}}}^{1t}^{3x_i}}{\delta_3 x_i}. \tag{108}$$

Spatially sixth- and higher-order schemes are also constructed in the same manner as in Morinishi et al.[1,4]. Arrangement for a non-uniform staggered grid is done in the same way as in Appendix B and Morinishi et al.[4]. Corresponding high-order treatment for the viscous term and recommendable boundary treatment are undertaken in the same way as in Desjardins et al. [7].

5. Semi-discrete convection schemes

For semi-discrete schemes considered in this section, the spatio-temporal grid in Fig. 1(b) is replaced by Fig. 2.

Semi-discrete fully conservative finite difference schemes in a staggered grid system are written as $(Cont.-S2)$, $(Div.-S2)_i$, $(Cont.-S4)$, $(Div.-S4)_i$, etc., which are the exclusions of the temporal discretization operators from $(Cont.-FS2)$, $(Div.-FS2)_i$, $(Cont.-FS4_2)$, $(Div.-FS4_2)_i$, etc., respectively. For instance, the fourth-order accurate semi-discrete schemes for the left-hand side of the continuity and the convection forms of the momentum equation are

$$\begin{aligned} (Cont.-S4) &\equiv \frac{d \rho}{dt} + \frac{9}{8} \frac{\delta_1 \overline{\overline{\overline{\overline{\rho}}}}^{4thx_j} u_j}{\delta_1 x_j} - \frac{1}{8} \frac{\delta_3 \overline{\overline{\overline{\overline{\rho}}}}^{4thx_j} u_j}{\delta_3 x_j} (= 0), \\ (Div.-S4)_i &\equiv \frac{d \overline{\overline{\overline{\overline{\rho}}}}^{4thx_i} u_i}{dt} + \frac{9}{8} \frac{\delta_1 \overline{\overline{\overline{\overline{\rho}}}}^{4thx_j} u_j \overline{\overline{\overline{\overline{\rho}}}}^{4thx_i} \widehat{u}_i^{1x_j}}{\delta_1 x_j} - \frac{1}{8} \frac{\delta_3 \overline{\overline{\overline{\overline{\rho}}}}^{4thx_j} u_j \overline{\overline{\overline{\overline{\rho}}}}^{4thx_i} \widehat{u}_i^{3x_j}}{\delta_3 x_j}, \\ (Adv.-S4)_i &\equiv \overline{\overline{\overline{\overline{\rho}}}}^{4thx_i} \frac{d u_i}{dt} + \frac{9}{8} \frac{\overline{\overline{\overline{\overline{\rho}}}}^{4thx_j} \delta_1 u_i \overline{\overline{\overline{\overline{\rho}}}}^{1x_j}}{\delta_1 x_j} - \frac{1}{8} \frac{\overline{\overline{\overline{\overline{\rho}}}}^{4thx_j} \delta_3 u_i \overline{\overline{\overline{\overline{\rho}}}}^{3x_j}}{\delta_3 x_j}, \\ (Skew.-S4)_i &\equiv \sqrt{\overline{\overline{\overline{\overline{\rho}}}}^{4thx_i}} \frac{d \sqrt{\overline{\overline{\overline{\overline{\rho}}}}^{4thx_i}} u_i}{dt} + \frac{1}{2} \left(\frac{9}{8} \frac{\delta_1 \overline{\overline{\overline{\overline{\rho}}}}^{4thx_j} u_j \overline{\overline{\overline{\overline{\rho}}}}^{4thx_i} \widehat{u}_i^{1x_j}}{\delta_1 x_j} - \frac{1}{8} \frac{\delta_3 \overline{\overline{\overline{\overline{\rho}}}}^{4thx_j} u_j \overline{\overline{\overline{\overline{\rho}}}}^{4thx_i} \widehat{u}_i^{3x_j}}{\delta_3 x_j} \right) \\ &\quad + \frac{1}{2} \left(\frac{9}{8} \frac{\overline{\overline{\overline{\overline{\rho}}}}^{4thx_j} \delta_1 u_i \overline{\overline{\overline{\overline{\rho}}}}^{1x_j}}{\delta_1 x_j} - \frac{1}{8} \frac{\overline{\overline{\overline{\overline{\rho}}}}^{4thx_j} \delta_3 u_i \overline{\overline{\overline{\overline{\rho}}}}^{3x_j}}{\delta_3 x_j} \right). \end{aligned}$$

The fourth-order accurate convection schemes above are equivalent if $(Cont.-S4) = 0$ and time marching error is negligible. The semi-discrete schemes of the convection forms of the internal energy equation and the pressure-related terms are defined in the same way. The schemes for divergence and advective forms are straightforward extensions of the fourth-order accurate schemes for incompressible flow by Morinishi et al. [1], and have already been used in Nicoud [6] and Desjardins

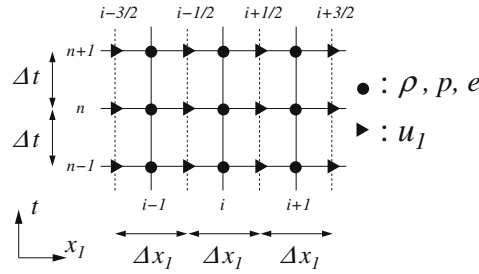


Fig. 2. Spatio-temporal grid for semi-discrete schemes. i and n are spatio-temporal location indices.

et al. [7]. Note that the temporal derivative term is included in each form in the present study, which is one of the important points for the construction of a set of commutable convection schemes for compressible flow. Even for semi-discrete methods, the present skew-symmetric form seems to be the first in the literature to the author’s knowledge.

For compressible flow simulations at a low-Mach number, a compact finite difference has been used as a high-order spatial discretization method after Lele [23]. However, the convection schemes with the compact finite difference are in general not commutable with each other even if the corresponding discrete continuity is satisfied, and none of the fully conservative convection scheme with the compact finite difference seems to exist. This means that the choice of the form of convection is definite for the reliability of the simulation with the compact finite difference. The rest of this section concentrates on the construction of a semi-discrete convection scheme with a compact finite difference in a staggered grid system. For the reader’s convenience, the compact finite difference scheme in a regular grid system is presented in Appendix A.2.

5.1. Mid-point compact finite difference

It is natural to introduce the mid-point compact finite difference and interpolation to the schemes in a staggered grid system [24]. The n -th order accurate mid-point compact finite difference in x_1 direction up to $n = 8$, $\delta_{c_n} \phi / \delta_{c_n} x_1$, is obtained by solving the following tri-diagonal system [23]:

$$\alpha \frac{\delta_{c_n} \phi}{\delta_{c_n} x_1} \Big|_{i-1,j,k} + \frac{\delta_{c_n} \phi}{\delta_{c_n} x_1} \Big|_{i,j,k} + \alpha \frac{\delta_{c_n} \phi}{\delta_{c_n} x_1} \Big|_{i+1,j,k} = A \frac{\delta_1 \phi}{\delta_1 x_1} \Big|_{i,j,k} + B \frac{\delta_3 \phi}{\delta_3 x_1} \Big|_{i,j,k} + C \frac{\delta_5 \phi}{\delta_5 x_1} \Big|_{i,j,k}. \tag{109}$$

A general sixth-order compact finite difference is given by $A = (225 - 206\alpha)/192$, $B = (414\alpha - 25)/128$, and $C = (9 - 62\alpha)/384$. $\alpha = 9/62$ is the most compact sixth-order compact finite difference. The eighth-order formula is obtained with $\alpha = 75/354$. The n -th order accurate compact interpolation in x_1 direction up to $n = 8$, $\bar{\phi}^{c_n x_1}$, is also obtained by solving the following tri-diagonal system:

$$\bar{\alpha} \bar{\phi}^{c_n x_1} \Big|_{i-1,j,k} + \bar{\phi}^{c_n x_1} \Big|_{i,j,k} + \bar{\alpha} \bar{\phi}^{c_n x_1} \Big|_{i+1,j,k} = \bar{A} \bar{\phi}^{1x_1} \Big|_{i,j,k} + \bar{B} \bar{\phi}^{3x_1} \Big|_{i,j,k} + \bar{C} \bar{\phi}^{5x_1} \Big|_{i,j,k}. \tag{110}$$

A general sixth-order compact interpolation is given by $\bar{A} = (75 + 70\bar{\alpha})/64$, $\bar{B} = (126\bar{\alpha} - 25)/128$, and $\bar{C} = (3 - 10\bar{\alpha})/128$. $\bar{\alpha} = 3/10$ is the most compact sixth-order compact interpolation. The eighth-order formula is obtained with $\bar{\alpha} = 5/14$. The compact difference and interpolation in x_2 and x_3 directions are defined in the same way as for x_1 direction.

5.2. Compact finite difference schemes in a staggered grid system

The left-hand side of the continuity is discretized with the compact finite difference and interpolation in a staggered grid system as

$$(Cont.-SCn) \equiv \frac{d\rho}{dt} + \frac{\delta_{c_n} \bar{\rho}^{c_n x_j} u_j}{\delta_{c_n} x_j} (= 0), \tag{111}$$

where $-SCn$ denotes a n -th order accurate compact scheme in a staggered grid system. For instance, $-SC6$ stands for a sixth-order accurate compact scheme in a staggered grid system. The schemes of the three convection forms for the momentum equation are as follows:

$$(Div.-SCn)_i \equiv \frac{d \bar{\rho}^{c_n x_i} u_i}{dt} + \frac{\delta_{c_n} \bar{\rho}^{c_n x_j} u_j}{\delta_{c_n} x_j} \bar{u}_i^{c_n x_j}, \tag{112}$$

$$(Adv.-SCn)_i \equiv \bar{\rho}^{c_n x_i} \frac{du_i}{dt} + \frac{\bar{\rho}^{c_n x_j} \delta_{c_n} u_i}{\delta_{c_n} x_j} \bar{u}_j^{c_n x_j}, \tag{113}$$

$$(Skew.-SCn)_i \equiv \sqrt{\bar{\rho}^{c_n x_i}} \frac{d \sqrt{\bar{\rho}^{c_n x_i}} u_i}{dt} + \frac{1}{2} \left(\frac{\delta_{c_n} \bar{\rho}^{c_n x_j} u_j}{\delta_{c_n} x_j} \bar{u}_i^{c_n x_j} + \frac{\bar{\rho}^{c_n x_j} \delta_{c_n} u_i}{\delta_{c_n} x_j} \bar{u}_j^{c_n x_j} \right). \tag{114}$$

The three convection forms for the internal energy equation are discretized as

$$(Div.-SCn)_e \equiv \frac{d\rho e}{dt} + \frac{\delta_{c_n} \bar{\rho}^{c_n x_j} u_j \bar{e}^{c_n x_j}}{\delta_{c_n} x_j}, \tag{115}$$

$$(Adv.-SCn)_e \equiv \rho \frac{de}{dt} + \bar{\rho}^{c_n x_j} u_j \frac{\delta_{c_n} e^{c_n x_j}}{\delta_{c_n} x_j}, \tag{116}$$

$$(Skew.-SCn)_e \equiv \sqrt{\rho} \frac{d\sqrt{\rho} e}{dt} + \frac{1}{2} \left(\frac{\delta_{c_n} \bar{\rho}^{c_n x_j} u_j \bar{e}^{c_n x_j}}{\delta_{c_n} x_j} + \overline{\bar{\rho}^{c_n x_j} u_j \frac{\delta_{c_n} e^{c_n x_j}}{\delta_{c_n} x_j}} \right). \tag{117}$$

The pressure term in the momentum equation and the pressure-dilatation term in the internal energy equation are discretized as follows:

$$(Pres.-SCn)_i \equiv \frac{\delta_{c_n} p}{\delta_{c_n} x_i}, \tag{118}$$

$$(PD.-SCn)_e \equiv p \frac{\delta_{c_n} u_i}{\delta_{c_n} x_i}. \tag{119}$$

Note that the set of convection schemes with the n -th order accurate compact finite difference are in general not commutable even if the corresponding discrete continuity, $(Cont.-SCn) = 0$, is satisfied. Nevertheless, the analysis is interesting because of the prospect for the numerical stability with the present skew-symmetric form.

6. Numerical tests

6.1. Time marching methods

A third-order Runge–Kutta method [25] is used for time advancement of the semi-discrete equations for mass, momentum and internal energy in Section 5. The transport equations with divergence, advective, and skew-symmetric forms of convection are advanced, respectively, with the following procedures:

$$\begin{aligned} \frac{d(\rho\phi)}{dt} &= R_\phi^D \rightarrow (\rho\phi)^{n+1} \rightarrow \phi^{n+1} = (\rho\phi)^{n+1} / \rho^{n+1}, \\ \frac{d\phi}{dt} &= \frac{1}{\rho} R_\phi^A \rightarrow \phi^{n+1}, \\ \frac{d(\sqrt{\rho}\phi)}{dt} &= \frac{1}{\sqrt{\rho}} R_\phi^S \rightarrow (\sqrt{\rho}\phi)^{n+1} \rightarrow \phi^{n+1} = (\sqrt{\rho}\phi)^{n+1} / \sqrt{\rho^{n+1}}, \end{aligned}$$

where R_ϕ^D , R_ϕ^A , and R_ϕ^S are the right-hand sides of the corresponding equations. The pressure is estimated using the equation of state in simulations with semi-discrete schemes.

On the other hand, the fully discrete finite difference schemes proposed in Section 4 require a robust solver for the non-linear discrete system. In this study, the non-linear system of fully discrete equations is solved using the Jacobian-free Newton-Krylov (JFNK) method [26,27] with the flexible preconditioning GMRES(m) method [28,29] as the Krylov inner solver, where m is the period of restarted GMRES method and m of 30 is used. In the non-linear solver, pressure, velocity, and internal energy are selected as the components of the solution vector. The choice of pressure as one of the solution vector components corresponds to the pressure-based method in which the pressure Helmholtz equation is solved [17,18]. The density is estimated using the equation of state. The non-linear solver may be replaced by the Helmholtz method with some modifications for practical problems.

6.2. Periodic inviscid flow

To demonstrate the fully conservative property of the present schemes with numerical test, inviscid flow simulations are performed on a three-dimensional periodic domain. This is very simple but is an ideal test for the secondary conservation property of convection schemes. The analytical conservation requirements dictate that the mass, momentum and total energy should be conserved in time, while the mass, momentum, and internal energy equations are solved. The periodic region is $L_0 \times L_0 \times L_0$ ($L_0 = 1$), and $10 \times 10 \times 10$ mesh is used. Solenoidal initial velocity fields are generated from a vector potential constructed from a set of uniform random numbers. The initial velocity fields are then normalized as $\langle u_1 \rangle = \langle u_2 \rangle = \langle u_3 \rangle = 0$ and $\langle u_1^2 + u_2^2 + u_3^2 \rangle / 3 = u_0^2$, where $\langle \rangle$ indicates volumetric average. The initial thermodynamic variables are uniformly set to $\rho/\rho_0 = 1$, $e/u_0^2 = 1/[\gamma(\gamma - 1)M_0^2]$, and $p/(\rho_0 u_0^2) = 1/(\gamma M_0^2)$, where $M_0 = u_0/c_0 = 0.2$ is the initial Mach number. The thermodynamic conditions correspond to $e/e_0 = 1$ and $p/p_0 = 1$, where $c_0 = [\gamma\rho_0/p_0]^{1/2} = [\gamma(\gamma - 1)e_0]^{1/2}$ is the initial speed of sound.

Table 1 shows the relative error of total energy, $\varepsilon_E \equiv (\langle \rho E \rangle - \langle \rho E \rangle_0) / \langle \rho E \rangle_0$, for several semi-discrete schemes in a staggered grid system with RK3 after an integration time of $t_{u_0}/L_0 = 10$. Time increment of $\Delta t u_0/L_0 = 0.002$ corresponds to the initial Courant number of 0.16, which is lower than the stability limit of $C < 1.73$ for RK3. The semi-discrete fully con-

Table 1

Total energy conservation error for semi-discrete schemes with RK3. $\Delta t u_0 / L_0 = 0.002$.

Convection schemes	ϵ_E at $tu_0/L_0 = 10$
(Div.-S2)	-3.275×10^{-5}
(Adv.-S2)	-7.274×10^{-5}
(Skew.-S2)	-6.689×10^{-5}
(Div.-S4)	-6.296×10^{-5}
(Adv.-S4)	-1.377×10^{-4}
(Skew.-S4)	-1.276×10^{-4}
(Div.-SC6)	Blow up
(Adv.-SC6)	Blow up
(Skew.-SC6)	-1.171×10^{-3}

servative second- and fourth-order schemes with the divergence forms, (Div.-S2) and (Div.-S4), conserve total energy to within the time marching error. The corresponding semi-discrete schemes with advective and skew-symmetric forms, (Adv.-S2), (Skew.-S2), (Adv.-S4), and (Skew.-S4), are also seen to be conservative. The results of the sixth-order accurate compact finite difference method ($\alpha = 9/62$, $\bar{\alpha} = 3/10$) with the divergence and advective forms, (Div.-SC6) and (Adv.-SC6), diverge. The only stable case with the compact finite difference method is the one with the skew-symmetric form of convection, (Skew.-SC6). This reveals that a stable simulation with high-order compact finite difference is possible with the skew-symmetric form of convection without any stabilization technique like low-pass filtering.

Table 2 shows the relative total energy error for several fully discrete schemes in a staggered grid system. The fully discrete fully conservative second-order accurate schemes, (Div.-FS2), (Adv.-FS2), and (Skew.-FS2), conserve total energy to within the round-off error of computer, which demonstrates the complete commutability and conservation property of the present schemes. The fully discrete fully conservative spatially fourth-order accurate schemes, (Div.-FS4₂), (Adv.-FS4₂), and (Skew.-FS4₂), also conserve total energy to within the round-off error. In this table, (Div.-FS2')_i is the convection scheme with divergence form, where \bar{u}_i in (68) is replaced by \bar{u}_i^{-1t} ,

$$(Div.-FS2')_i \equiv \frac{\delta_1 \bar{\rho}^{-1x_i} u_i}{\delta_1 t} + \frac{\delta_1 \bar{g}_j^{-1x_i} \bar{u}_i^{-1x_j}}{\delta_1 x_j}, \tag{120}$$

which corresponds to the fully discrete convection scheme in Pierce et al. [17] and Wall et al. [18]. As mentioned by Pierce et al. [17], this convection scheme has a secondary conservation error of $O(\Delta t^2)$. Note that the time marching method used in the above convection scheme is not the Crank–Nicolson method but an implicit mid-point method which is equivalent to the one-stage second-order accurate implicit Runge–Kutta (IRK2) method. Therefore, the time marching method in the fully discrete fully conservative schemes in Section 4 is regarded as a modified implicit mid-point method.

Fig. 3 shows the relative total energy error at $tu_0/L_0 = 10$ as a function of the time increment for several schemes. As expected, the time stepping error decreases with the cube of Δt for the semi-discrete schemes with RK3. The error of (Div.-FS2') decreases with the square of Δt , which demonstrates numerically the estimation of Pierce et al. [17]. On the other hand, the errors of (Div.-FS2) and (Div.-FS4₂) retain the order of a computer round-off error as long as the non-linear solver works. Indeed, the Courant number for $\Delta t u_0 / L_0 = 0.1$ is over 8.

6.3. Compressible isotropic turbulence

The second numerical test validates the fully discrete fully conservative second-order accurate scheme in Section 4 for viscous flow by performing DNS of compressible isotropic turbulence on a 64^3 grid with $Re_\lambda = 30$ and $M_{t_0} = 0.3$, where $Re_\lambda \equiv \rho_0 u_0 \lambda / \mu_0$ and $M_{t_0} \equiv \sqrt{3} u_0 / c_0$. The periodic computational box is $2\pi L_0 \times 2\pi L_0 \times 2\pi L_0$. The solenoidal initial velocity field is generated with a spectrum distribution [30] of

Table 2

Total energy conservation error for fully discrete schemes. $\Delta t u_0 / L_0 = 0.002$.

Convection schemes	ϵ_E at $tu_0/L_0 = 10$
(Div.-FS2)	-3.526×10^{-14}
(Adv.-FS2)	-1.266×10^{-13}
(Skew.-FS2)	-3.009×10^{-13}
(Div.-FS4 ₂)	-1.355×10^{-14}
(Adv.-FS4 ₂)	-3.425×10^{-13}
(Skew.-FS4 ₂)	-2.541×10^{-13}
(Div.-FS2')	$+2.110 \times 10^{-7}$

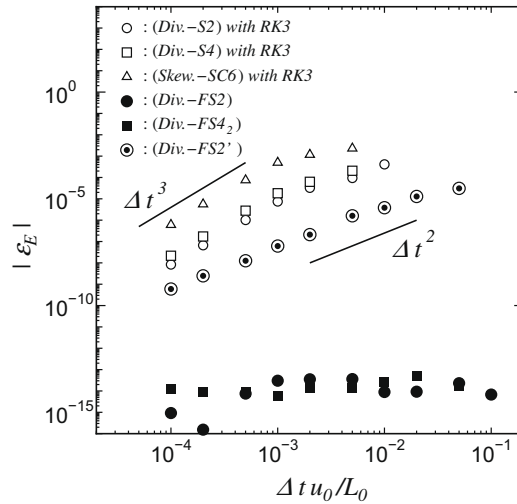


Fig. 3. Total energy conservation error as a function of time increment for fully and semi-discrete schemes. Semi-discrete schemes are integrated with RK3.

$$E(k) = 16 \sqrt{\frac{2}{\pi}} \frac{u_0^2}{k_p} \left(\frac{k}{k_p}\right)^4 e^{-2k^2/k_p^2}, \tag{121}$$

where the peak wavenumber is set to $k_p = 4/L_0$. The large eddy turnover time for this spectrum is $\tau = 2/(k_p u_0)$. The initial Taylor microscale of the flow was $\lambda \equiv [\langle u_1'^2 \rangle / \langle (\partial u_1' / \partial x_1)^2 \rangle]^{1/2} \sim 0.5L_0$. The thermodynamic variables are uniformly set to $\rho/\rho_0 = 1$, $e/u_0^2 = 3/[\gamma(\gamma - 1)M_{t_0}^2]$, and $p/(\rho_0 u_0^2) = 3/(\gamma M_{t_0}^2)$. These conditions correspond to $e/e_0 = 1$ and $p/p_0 = 1$, where $c_0 = [\gamma p_0 / \rho_0]^{1/2} = [\gamma(\gamma - 1)e_0]^{1/2}$ is the initial speed of sound. A time increment of $\Delta t/\tau = 0.02$ corresponds to the Courant number around 1.0.

The evolution of turbulence kinetic energy and thermodynamic variable fluctuations are show in Fig. 4. The various fluctuation quantities are defined by: $K \equiv \langle u_1'^2 + u_2'^2 + u_3'^2 \rangle / 2$, $p'_{rms} \equiv \langle p'^2 \rangle^{1/2}$, $v'_{rms} \equiv \langle (1/\rho)^{\prime 2} \rangle^{1/2}$, and $e'_{rms} \equiv \langle e'^2 \rangle^{1/2}$. In the figure,

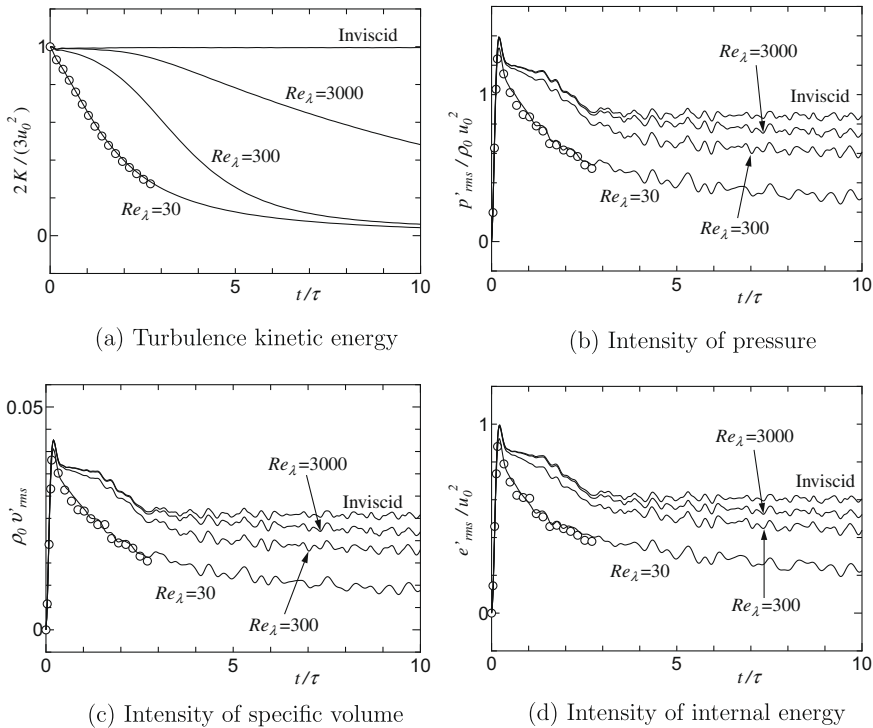


Fig. 4. Compressible isotropic turbulence with the second-order fully discrete fully conservative scheme proposed in Section 4. \circ are the de-aliased spectral DNS data at $Re_\lambda = 30$ in [19].

○ are the de-aliased spectral DNS data in [19] with $Re_\lambda = 30$ and $M_{t_0} = 0.3$ with the corresponding initial condition. The present $Re_\lambda = 30$ simulation is regarded as a DNS and very good agreement with the referenced DNS data is observed. The present simulations except $Re_\lambda = 30$ are unresolved and are carried out in order to check the non-linear numerical stability of the scheme for viscous flow. The fluctuation intensities increase with increasing Re_λ , however, the values are bounded at those for the inviscid simulation ($Re_\lambda = \infty$). Even for the inviscid case the simulation is stable for the present initial condition.

6.4. Open cavity flow

The third numerical test is done on the simulation of a periodic two dimensional channel flow with an open cavity, in which the streamwise grid spacings around the vertical cavity wall lines are fine as shown in Fig. 5. The flow field is composed of periodic main channel of $5h \times 2h$ and a shallow open cavity of $2h \times h/2$ and is bounded with upper and lower isothermal walls. The grid numbers in the main channel and open cavity are 260×100 and 100×50 , respectively. The grid spacings adjacent to the walls are set to $h/200$. The Reynolds number based on the half main channel height $Re_h \equiv \rho_0 U_c h / \mu_0$ is set to 800 or 1200, where U_c is the centerline velocity of laminar basic solution for the plane channel. The periodic flow is driven by the streamwise non-dimensional uniform body force of $-2/Re_h$. The Mach number based on the centerline velocity and internal energy on the walls is $M_c \equiv U_c / c_0 = 0.2$, where $c_0 = [\gamma(\gamma - 1)e_0]^{1/2}$ and e_0 is internal energy on the walls. The initial velocity profile in the main channel is the basic solution for the laminar plane channel. The initial thermodynamic variables are uniformly set to $\rho/\rho_0 = 1$, $e/U_c^2 = 1/[\gamma(\gamma - 1)M_c^2]$, and $p/(\rho_0 U_c^2) = 1/(\gamma M_c^2)$.

The simulation is carried out using the fully discrete fully conservative second-order accurate finite difference scheme in the non-uniform staggered grid system presented in Appendix B. Stable simulations were possible with a non-dimensional time increment of $U_c \Delta t / h = 0.01$. The corresponding maximum Courant number is about $C = 12$, which demonstrates the robustness of the scheme for simulations with stretching mesh like Fig. 5. Fig. 6 shows the temporal evolution of bulk veloc-

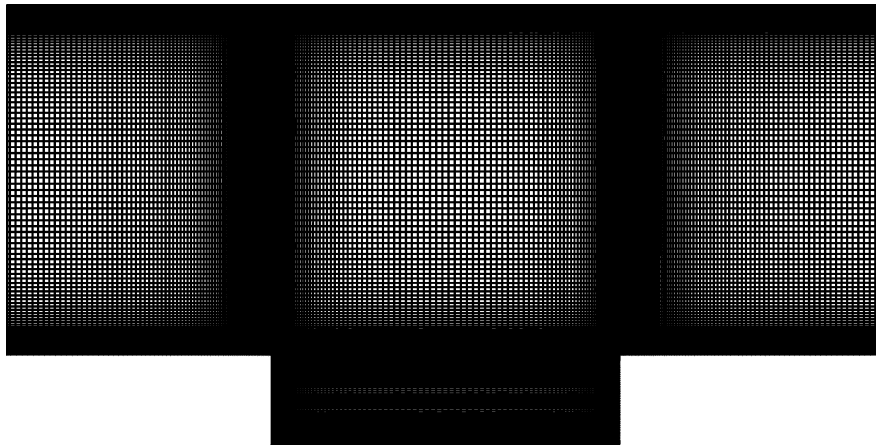


Fig. 5. Numerical mesh for open cavity flow simulation.

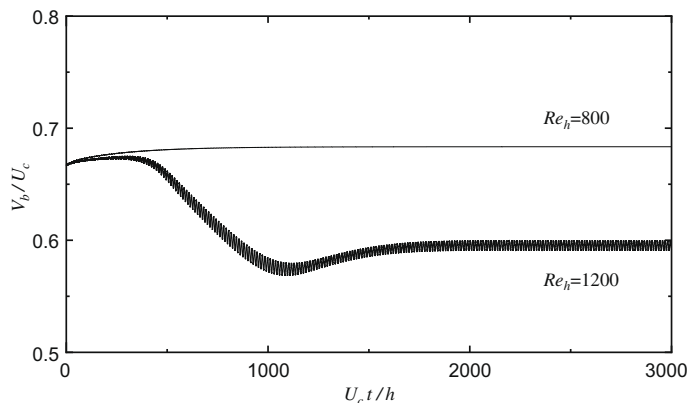
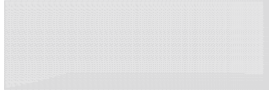


Fig. 6. Evolution of bulk velocity at a section of main channel.



ity V_b at a main channel section. From the consideration of incompressible flow [31] the critical Reynolds number is around 1000, and the numbers of 800 and 1200 correspond to subcritical and supercritical regimes, respectively. From Fig. 6 the flow is steady for $Re_h = 800$. On the other hand, the instability is shown to result in stationary self sustained flow oscillations after an initial transient period of $U_c t/h = 1500$ for $Re_h = 1200$, and the critical behavior for the incompressible flow is recovered in the compressible flow simulations. Figs. 7 and 8 are iso-vorticity lines for $Re_h = 800$ and 1200, respectively, at $U_c t/h = 2400$. The flow at $Re_h = 800$ is subcritical, and the vorticity in the cavity is almost steady. On the other hand, the flow at $Re_h = 1200$, the self-sustained flow oscillation, leads to the waviness and roll-up patterns in the free shear layer at the cavity edge.

7. Conclusion

The form of convective terms for the transport equations of compressible flow is discussed. Commutable divergence, advective, and skew-symmetric forms of convective term are defined by including the temporal derivative term for compressible flow. These forms are analytically equivalent if the continuity is satisfied. The skew-symmetric form is secondary conservative, while the divergence form is primary conservative, without the aid of the continuity. Conservations of mass, momentum, and total energy for compressible flow are also specified as analytical requirements for a proper set of discrete equations. In addition to the constraint for the convective term, the requirement for the pressure-related terms in the momentum and internal energy equations is specified, since total energy is the sum of kinetic and internal energies. Then,

fully discrete fully conservative finite difference schemes are derived by introducing the square-root density weighted interpolation, in which the analytical requirements are discretely satisfied. The schemes of divergence, advective, and skew-symmetric forms of convection are commutable if the corresponding discrete continuity is satisfied, and the divergence and skew-symmetric schemes are, respectively, primary and secondary conservative, without the aid of the discrete continuity. In addition, the convection scheme based on the skew-symmetric form suitable for compact finite difference is presented. The conservation properties of the present schemes are demonstrated numerically in a periodic inviscid flow. DNS of compressible isotropic turbulence and two-dimensional open cavity flow are also performed using the present fully discrete fully conservative second-order scheme.

Acknowledgments

This work was supported by Grants-in-Aid for Scientific Research B (No. 18360087, No. 21360081) and Grant-in-Aid for Exploratory Research (No. 20656035) from Japan Society for the Promotion of Science. The author also expresses gratitude for the assistance with the numerical tests generously provided by Mr. Y. Sugiyama and Mr. M. Yamaki.

Appendix A. Schemes in a regular grid system

A.1. Fully conservative finite difference scheme in a regular grid system

This subsection presents the fully conservative finite difference scheme in a spatially regular and temporally staggered grid system as shown in Fig. 9. In this arrangement, spatial distribution of variables is collocated as shown in Fig. 9(a). Temporal staggering (Fig. 9(b)) is recommended for suitable discretization of the continuity.

The fully discrete fully conservative second-order accurate finite difference schemes in a regular grid system for (20)–(23) are as follows:

$$(Cont. - FR2) = 0, \tag{122}$$

$$(Conv. - FR2)_i + (Pres.-FR2)_i = \frac{\delta_2 \tau_{ij}}{\delta_2 x_j}, \tag{123}$$

$$(Conv. - FR2)_e + (PD.-FR2)_e = \tau_{ij} \frac{\delta_2 \hat{u}_i}{\delta_2 x_j} - \frac{\delta_2 q_j}{\delta_2 x_j}, \tag{124}$$

$$\text{with } \bar{p}^{1t} = p(\bar{p}^{1t}, e), \text{ or } \bar{p}^{1t} = \rho(\bar{p}^{1t}, e), \text{ or } e = e(\bar{p}^{1t}, \bar{p}^{1t}), \tag{125}$$

where inviscid terms are denoted symbolically and *-FR2* denotes a fully discrete second-order accurate approximation in a regular grid system. *(Cont. - FR2)* is the left-hand side of the continuity:

$$(Cont. - FR2) \equiv \frac{\delta_1 \rho}{\delta_1 t} + \frac{\delta_1 g_j}{\delta_1 x_j} (= 0), \tag{126}$$

where g_j is the numerical mass flux for the second-order accurate schemes in a regular grid system defined by

$$g_j \equiv \bar{\rho}^{1t} u_j^{1x_j}. \tag{127}$$

$(Conv. - FR2)_\phi$ is a generic form of convection scheme for the transport equation of ϕ , and takes one of the following forms for $\phi = u_i$ and e :

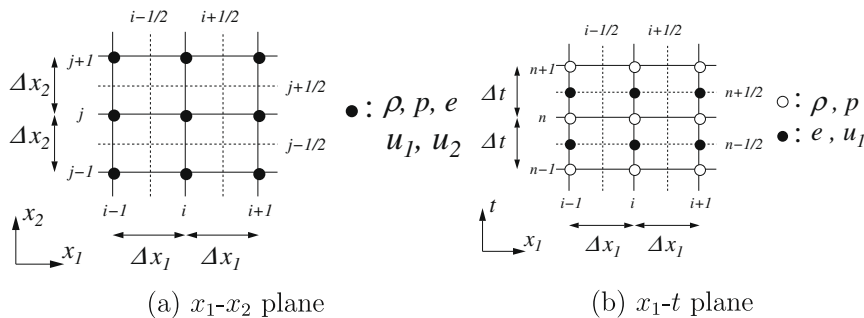


Fig. 9. Spatially regular and temporally staggered grid system. *i, j,* and *n* are spatio-temporal location indices.

$$(Div.-FR2)_\phi \equiv \frac{\delta_1 \bar{\rho}^{1t} \phi}{\delta_1 t} + \frac{\delta_1 \bar{g}_j^{1t} \widehat{\phi}^{1x_j}}{\delta_1 x_j}, \quad (128)$$

$$(Adv.-FR2)_\phi \equiv \bar{\rho}^{1t} \frac{\delta_1 \phi}{\delta_1 t} + (\bar{\phi}^{1t} - \widehat{\phi}) \frac{\delta_1 \bar{\rho}^{1t}}{\delta_1 t} + \bar{g}_j^{1t} \frac{\delta_1 \widehat{\phi}^{1x_j}}{\delta_1 x_j}, \quad (129)$$

$$(Skew.-FR2)_\phi \equiv \sqrt{\bar{\rho}^{1t}} \frac{\delta_1 \sqrt{\bar{\rho}^{1t}} \phi}{\delta_1 t} + \frac{1}{2} \left(\frac{\delta_1 \bar{g}_j^{1t} \widehat{\phi}^{1x_j}}{\delta_1 x_j} + \overline{\bar{g}_j^{1t} \frac{\delta_1 \widehat{\phi}^{1x_j}}{\delta_1 x_j}} \right). \quad (130)$$

Here, the convection schemes for the momentum equation ($\phi = u_i$) are abbreviated like $(Conv.-FR2)_i$, $(Div.-FR2)_i$, and so on. $\widehat{\phi}$ is the square-root density weighted interpolation for the regular grid system.

$$\widehat{\phi} \equiv \frac{\sqrt{\bar{\rho}^{1t}} \phi}{\sqrt{\bar{\rho}^{1t}}}. \quad (131)$$

$(Pres.-FR2)_i$ and $(PD.-FR2)_e$ are the discrete pressure term in the momentum equation and the discrete pressure-dilatation term in the internal energy equation defined, respectively, by

$$(Pres.-FR2)_i \equiv \frac{\delta_2 \bar{p}^{1t}}{\delta_2 x_i}, \quad (132)$$

$$(PD.-FR2)_e \equiv \bar{p}^{1t} \frac{\delta_2 \widehat{u}_i}{\delta_2 x_i}. \quad (133)$$

Commutability between the schemes for divergence and advective forms in a regular grid system is demonstrated using (56), (58) and (59) as follows:

$$(Div.-FR2)_\phi = (Adv.-FR2)_\phi + \widehat{\phi} \overline{(Cont.-FR2)^{1t}}. \quad (134)$$

The relation for the skew-symmetric form in a regular grid system is demonstrated using (59), (60) and (134) as

$$\begin{aligned} (Skew.-FR2)_\phi &= \frac{1}{2} (Div.-FR2)_\phi + \frac{1}{2} (Adv.-FR2)_\phi = (Div.-FR2)_\phi - \frac{1}{2} \widehat{\phi} \overline{(Cont.-FR2)^{1t}} \\ &= (Adv.-FR2)_\phi + \frac{1}{2} \widehat{\phi} \overline{(Cont.-FR2)^{1t}}. \end{aligned} \quad (135)$$

The secondary conservation property of the skew-symmetric scheme is also demonstrated using (57) and (60) as

$$\widehat{\phi} (Skew.-FR2)_\phi = \frac{\delta_1 \bar{\rho}^{1t} \phi^2 / 2}{\delta_1 t} + \frac{\delta_1 \bar{g}_j^{1t} \widehat{\phi} \widehat{\phi}^{1x_j} / 2}{\delta_1 x_j}. \quad (136)$$

The convective term of the total energy equation obtained as a result is written using (57) and (60) as

$$\widehat{u}_i (Skew.-FR2)_i + (Div.-FR2)_e = \frac{\delta_1 (\rho E)_{FR2}}{\delta_1 t} + \frac{\delta_1}{\delta_1 x_j} \left(\frac{1}{2} \bar{g}_j^{1t} \widehat{u}_i \widehat{u}_i^{1x_j} + \bar{g}_j^{1t} \bar{e}^{1x_j} \right), \quad (137)$$

where the discrete total energy norm conserved in the finite difference scheme is

$$(\rho E)_{FR2} \equiv \frac{1}{2} \bar{\rho}^{1t} u_i u_i + \bar{\rho}^{1t} e. \quad (138)$$

Note that the discrete total energy norm is uniquely defined in a regular grid system, since no spatial interpolation is required. Corresponding pressure terms in the kinetic energy and internal energy equations are merged into a conservative form in the total energy equation using (55).

$$\widehat{u}_i (Pres.-FR2)_i + (PD.-FR2)_e = \frac{\delta_1 \widehat{u}_i \bar{p}^{1t}}{\delta_1 x_i}. \quad (139)$$

Using (55), the viscous term is also conservative in the total energy equation:

$$\widehat{u}_i \frac{\delta_2 \tau_{ij}}{\delta_2 x_j} + \tau_{ij} \frac{\delta_2 \widehat{u}_i}{\delta_2 x_j} = \frac{\delta_1 \widehat{u}_i \tau_{ij}}{\delta_1 x_j}. \quad (140)$$

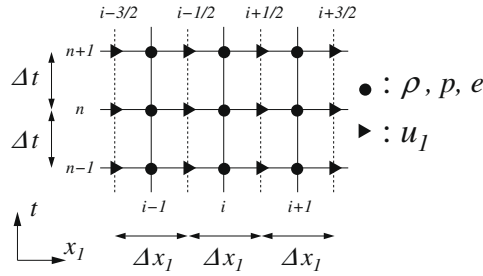


Fig. 10. Spatio-temporal grid for semi-discrete compact finite difference scheme in a regular grid. i and n are spatio-temporal location indices.

A.2. Semi-discrete compact finite difference scheme in a regular grid system

In this subsection, semi-discrete compact finite difference schemes are presented. For the compact finite difference schemes, the spatio-temporal grid in Fig. 9(b) is replaced by Fig. 10.

Even for a regular grid system, the use of the mid-point compact finite difference and interpolation is recommended [32]. This treatment offers a more stable computational method than that with the grid-point compact finite difference. The continuity is discretized as

$$(Cont. - RCn) \equiv \frac{d\rho}{dt} + \frac{\delta_{c_n} \overline{\rho u_j^{c_n x_j}}}{\delta_{c_n} x_j} (= 0), \tag{141}$$

where $-RCn$ denotes a n -th order accurate compact finite difference scheme in a regular grid system. The convection schemes for the divergence, advective and skew-symmetric forms are as follows:

$$(Div.-RCn)_\phi \equiv \frac{d\rho\phi}{dt} + \frac{\delta_{c_n} \overline{\rho u_j^{c_n x_j} \phi^{c_n x_j}}}{\delta_{c_n} x_j}, \tag{142}$$

$$(Adv.-RCn)_\phi \equiv \rho \frac{d\phi}{dt} + \overline{\rho u_j^{c_n x_j} \frac{\delta_{c_n} \phi^{c_n x_j}}{\delta_{c_n} x_j}}, \tag{143}$$

$$(Skew.-RCn)_\phi \equiv \sqrt{\rho} \frac{d\sqrt{\rho}\phi}{dt} + \frac{1}{2} \left(\frac{\delta_{c_n} \overline{\rho u_j^{c_n x_j} \phi^{c_n x_j}}}{\delta_{c_n} x_j} + \overline{\rho u_j^{c_n x_j} \frac{\delta_{c_n} \phi^{c_n x_j}}{\delta_{c_n} x_j}} \right). \tag{144}$$

Practically, only the skew-symmetric form of (144) is stable among (142)–(144) at the inviscid limit [32]. The schemes for the pressure term in the momentum equation and the pressure-dilatation term in the internal energy equation are as follows:

$$(Pres.-RCn)_i \equiv \frac{\overline{\delta_{c_n} p^{c_n x_i}}}{\delta_{c_n} x_i}, \tag{145}$$

$$(PD.-RCn)_e \equiv p \frac{\overline{\delta_{c_n} u_i^{c_n x_i}}}{\delta_{c_n} x_i}. \tag{146}$$

Appendix B. Fully discrete fully conservative finite difference scheme in a non-uniform staggered grid system

The extension of the fully discrete fully conservative finite difference scheme in Section 4.2 to a non-uniform grid is achieved by introducing the mapping of the independent variables from physical to computational spaces [33]. The discrete operations are acting on the corresponding uniform grid in the computational space [4]. One-dimensional mapping in each direction is introduced from the physical space (x_1, x_2, x_3) to the computational one (ξ_1, ξ_2, ξ_3) as

$$x_1 = x_1(\xi_1), \quad x_2 = x_2(\xi_2), \quad x_3 = x_3(\xi_3), \tag{147}$$

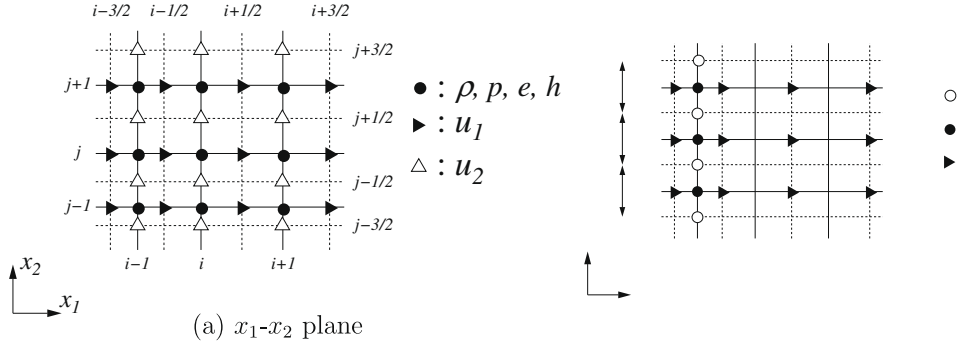
and

$$\xi_1 = \xi_1(x_1), \quad \xi_2 = \xi_2(x_2), \quad \xi_3 = \xi_3(x_3). \tag{148}$$

The scaling factor h_i and the transformation Jacobian J are defined from the relation:

$$h_1 = \frac{dx_1}{d\xi_1}, \quad h_2 = \frac{dx_2}{d\xi_2}, \quad h_3 = \frac{dx_3}{d\xi_3}, \quad J = h_1 h_2 h_3. \tag{149}$$

Correspondence between physical and computational spaces is shown in Figs. 11 and 12.



The governing Eqs. (20)–(23) are then represented in the computational space as:

$$(\text{Cont.}) = 0, \quad (150)$$

$$(\text{Conv.})_i + (\text{Pres.})_i = \frac{1}{J} \frac{\partial}{\partial \xi_j} \left(\frac{J}{h_j} \tau_{ij} \right), \quad (151)$$

$$(\text{Conv.})_e + (\text{PD.})_e = \frac{1}{J} \left(\frac{J}{h_j} \tau_{ij} \right) \frac{\partial u_i}{\partial \xi_j} - \frac{1}{J} \frac{\partial}{\partial \xi_j} \left(\frac{J}{h_j} q_j \right), \quad (152)$$

$$\text{with } p = p(\rho, e), \text{ or } \rho = \rho(p, e), \text{ or } e = e(\rho, p), \quad (153)$$

where (Cont.) is the left-hand side of the continuity defined by

$$(\text{Cont.}) \equiv \frac{\partial \rho}{\partial t} + \frac{1}{J} \frac{\partial}{\partial \xi_j} \left(\rho \frac{J}{h_j} u_j \right) (= 0). \quad (154)$$

$(\text{Conv.})_i$ is a generic form of convective term in the momentum equation in the computational space and takes one of the following forms:

$$(\text{Div.})_i \equiv \frac{1}{J} \frac{\partial J \rho u_i}{\partial t} + \frac{1}{J} \frac{\partial}{\partial \xi_j} \left\{ \left(\rho \frac{J}{h_j} u_j \right) u_i \right\}, \quad (155)$$

$$(\text{Adv.})_i \equiv \frac{1}{J} J \rho \frac{\partial u_i}{\partial t} + \frac{1}{J} \left(\rho \frac{J}{h_j} u_j \right) \frac{\partial u_i}{\partial \xi_j}, \quad (156)$$

$$(\text{Skew.})_i \equiv \frac{1}{J} \sqrt{J} \rho \frac{\partial \sqrt{J} \rho u_i}{\partial t} + \frac{1}{2J} \left[\frac{\partial}{\partial \xi_j} \left\{ \left(\rho \frac{J}{h_j} u_j \right) u_i \right\} + \left(\rho \frac{J}{h_j} u_j \right) \frac{\partial u_i}{\partial \xi_j} \right]. \quad (157)$$

$(\text{Conv.})_e$ is a generic form of convective term in the internal energy equation in the computational space and takes one of the following forms:

$$(Div.)_e \equiv \frac{\partial \rho e}{\partial t} + \frac{1}{J} \frac{\partial}{\partial \xi_j} \left\{ \left(\rho \frac{J}{h_j} u_j \right) e \right\}, \tag{158}$$

$$(Adv.)_e \equiv \rho \frac{\partial e}{\partial t} + \frac{1}{J} \left(\rho \frac{J}{h_j} u_j \right) \frac{\partial e}{\partial \xi_j}, \tag{159}$$

$$(Skew.)_e \equiv \sqrt{\rho} \frac{\partial \sqrt{\rho} e}{\partial t} + \frac{1}{2} \left[\frac{1}{J} \frac{\partial}{\partial \xi_j} \left\{ \left(\rho \frac{J}{h_j} u_j \right) e \right\} + \frac{1}{J} \left(\rho \frac{J}{h_j} u_j \right) \frac{\partial e}{\partial \xi_j} \right]. \tag{160}$$

(Pres.)_i and (PD.)_e are the pressure and pressure-dilatation terms in the computational space, respectively.

$$(Pres.)_i \equiv \frac{1}{J} \frac{J}{h_i} \frac{\partial p}{\partial \xi_i}, \tag{161}$$

$$(PD.)_i \equiv \frac{1}{J} p \frac{\partial}{\partial \xi_i} \left(\frac{J}{h_i} u_i \right). \tag{162}$$

Discrete operators acting in the computational space are defined as

$$\frac{\delta_m \phi}{\delta_m \xi_1} \Big|_{ij,k} \equiv \frac{\phi_{i+m/2,j,k} - \phi_{i-m/2,j,k}}{m \Delta \xi_1}, \tag{163}$$

$$\overline{\phi}^{m \xi_1} \Big|_{ij,k} \equiv \frac{\phi_{i+m/2,j,k} + \phi_{i-m/2,j,k}}{2}, \tag{164}$$

$$\widetilde{\phi \psi}^{m \xi_1} \Big|_{ij,k} \equiv \frac{\phi_{i+m/2,j,k} \psi_{i-m/2,j,k} + \psi_{i+m/2,j,k} \phi_{i-m/2,j,k}}{2}. \tag{165}$$

Discrete operators in ξ_2 and ξ_3 directions are defined in the same way as for ξ_1 direction, where the grid spacings in the computational space, $\Delta \xi_1$, $\Delta \xi_2$, and $\Delta \xi_3$, are supposed to be constant, and they are usually set to unity.

The governing equations in the computational space, (150)–(153), are then discretized as follows:

$$(Cont.-FS2) = 0, \tag{166}$$

$$(Conv.-FS2)_i + (Pres.-FS2)_i = \frac{1}{\overline{J}^{1 \xi_i}} \frac{\delta_1}{\delta_1 \xi_j} \odot \left(\frac{J}{h_j} \tau_{ij} \right), \tag{167}$$

$$(Conv.-FS2)_e + (PD.-FS2)_e = \frac{1}{J} \tau_{ij} \odot \left(\frac{J}{h_j} \frac{\delta_1 \hat{u}_i}{\delta_1 \xi_j} \right) - \frac{1}{J} \frac{\delta_1}{\delta_1 \xi_j} \left(\frac{J}{h_j} q_j \right), \tag{168}$$

$$\text{with } \overline{quadp}^{1t} = p(\overline{\rho}^{1t}, e), \quad \text{or} \quad \overline{\rho}^{1t} = \rho(\overline{p}^{1t}, e), \quad \text{or} \quad e = e(\overline{\rho}^{1t}, \overline{p}^{1t}). \tag{169}$$

(Cont.-FS2) is the left-hand side of the continuity and defined by

$$(Cont.-FS2) \equiv \frac{\delta_1 \rho}{\delta_1 t} + \frac{1}{J} \frac{\delta_1 G_j}{\delta_1 \xi_j} (= 0), \tag{170}$$

where G_j is the numerical contravariant mass flux in the computational space.

$$G_j \equiv \overline{\rho}^{1t \xi_j} \frac{J}{h_j} u_j. \tag{171}$$

(Conv.-FS2)_i is a generic form of convective term in the discrete momentum equation and takes one of the following schemes:

$$(Div.-FS2)_i \equiv \frac{1}{\overline{J}^{1 \xi_i}} \frac{\delta_1 \overline{\rho}^{1t \xi_i}}{\delta_1 t} u_i + \frac{1}{\overline{J}^{1 \xi_i}} \frac{\delta_1 \overline{G}_j^{1t \xi_i}}{\delta_1 \xi_j} \overline{\hat{u}}_i^{\xi_j}, \tag{172}$$

$$(Adv.-FS2)_i \equiv \frac{1}{\overline{J}^{1 \xi_i}} \frac{\delta_1 \overline{\rho}^{1t \xi_i}}{\delta_1 t} u_i + \frac{1}{\overline{J}^{1 \xi_i}} \left(\overline{u}_i^{1t} - \hat{u}_i \right) \frac{\delta_1 \overline{J}^{1t \xi_i}}{\delta_1 t} + \frac{1}{\overline{J}^{1 \xi_i}} \frac{\delta_1 \overline{\hat{u}}_i^{\xi_j}}{\delta_1 \xi_j}, \tag{173}$$

$$(Skew.-FS2)_i \equiv \frac{1}{\overline{J}^{1 \xi_i}} \frac{\delta_1 \sqrt{J \overline{\rho}^{1t \xi_i}}}{\delta_1 t} u_i + \frac{1}{2 \overline{J}^{1 \xi_i}} \left(\frac{\delta_1 \overline{G}_j^{1t \xi_i}}{\delta_1 \xi_j} \overline{\hat{u}}_i^{\xi_j} + \frac{\delta_1 \overline{\hat{u}}_i^{\xi_j}}{\delta_1 \xi_j} \overline{G}_j^{1t \xi_i} \right). \tag{174}$$

(Conv.-FS2)_e is a generic form of convective term in the discrete internal energy equation and takes one of the following schemes:

$$(Div.-FS2)_e \equiv \frac{\delta_1 \bar{\rho}^{1t} e}{\delta_1 t} + \frac{1}{J} \frac{\delta_1 \overline{G_j^{-1t} \bar{e}^{1\zeta_j}}}{\delta_1 \zeta_j}, \tag{175}$$

$$(Adv.-FS2)_e \equiv \overline{\bar{\rho}^{1t}} \frac{\delta_1 e}{\delta_1 t} + (\bar{e}^{1t} - \hat{e}) \frac{\delta_1 \bar{\rho}^{1t}}{\delta_1 t} + \frac{1}{J} \overline{G_j^{-1t} \frac{\delta_1 \bar{e}^{1\zeta_j}}{\delta_1 \zeta_j}}, \tag{176}$$

$$(Skew.-FS2)_e \equiv \sqrt{\overline{\bar{\rho}^{1t}}} \frac{\delta_1 \sqrt{\overline{\bar{\rho}^{1t}}} e}{\delta_1 t} + \frac{1}{2J} \left(\frac{\delta_1 \overline{G_j^{-1t} \bar{e}^{1\zeta_j}}}{\delta_1 \zeta_j} + \overline{G_j^{-1t} \frac{\delta_1 \bar{e}^{1\zeta_j}}{\delta_1 \zeta_j}} \right), \tag{177}$$

where \hat{u}_i and \hat{e} are the square-root density weighted velocity and internal energy interpolations in the computational space.

$$\hat{u}_i \equiv \frac{\sqrt{J \overline{\bar{\rho}^{1t} \zeta_i^{-1}}}}{\sqrt{J \overline{\bar{\rho}^{1t} \zeta_i^{-1}}}} u_i, \hat{e} \equiv \frac{\sqrt{\overline{\bar{\rho}^{1t}}}}{\sqrt{\overline{\bar{\rho}^{1t}}}} e. \tag{178}$$

The transformation Jacobian is appeared in the definition of the weighted interpolation of velocity for the non-uniform staggered grid arrangement. The pressure scheme, $(Pres.-FS2)_i$, and the pressure-dilatation scheme, $(PD.-FS2)_e$, are defined as follows:

$$(Pres.-FS2)_i \equiv \frac{1}{J^{1\zeta_i}} \frac{J}{\bar{h}_i} \frac{\delta_1 \overline{\bar{\rho}^{1t}}}{\delta_1 \zeta_i}, \tag{179}$$

$$(PD.-FS2)_e \equiv \frac{1}{J} \overline{\bar{\rho}^{1t}} \frac{\delta_1}{\delta_1 \zeta_i} \left(\frac{J}{\bar{h}_i} \hat{u}_i \right). \tag{180}$$

The commutability of the convection schemes and the secondary conservation property of the skew-symmetric form are demonstrated as follows:

$$(Div.-FS2)_i = (Adv.-FS2)_i + \frac{1}{J^{1\zeta_i}} \hat{u}_i \overline{J (Cont.-FS2)^{1\zeta_i}}, \tag{181}$$

$$\begin{aligned} (Skew.-FS2)_i &= \frac{1}{2} (Div.-FS2)_i + \frac{1}{2} (Adv.-FS2)_i = (Div.-FS2)_i - \frac{1}{2} \frac{1}{J^{1\zeta_i}} \hat{u}_i \overline{J (Cont.-FS2)^{1\zeta_i}} \\ &= (Adv.-FS2)_i + \frac{1}{2} \frac{1}{J^{1\zeta_i}} \hat{u}_i \overline{J (Cont.-FS2)^{1\zeta_i}}, \end{aligned} \tag{182}$$

$$\hat{u}_\alpha (Skew.-FS2)_\alpha = \frac{1}{J^{1\zeta_\alpha}} \frac{\delta_1 \overline{J \bar{\rho}^{1t} \zeta_\alpha}}{\delta_1 t} u_\alpha^2 / 2 + \frac{1}{J^{1\zeta_\alpha}} \frac{\delta_1 \overline{G_j^{-1t} \zeta_\alpha} \widehat{u}_\alpha \widehat{u}_\alpha^{1\zeta_j}}{\delta_1 \zeta_j} / 2, \tag{183}$$

where no summation is taken for the index α in the last equation. The commutability and secondary conservation property of the convection schemes for the internal energy equation are also demonstrated in the same way:

$$(Div.-FS2)_e = (Adv.-FS2)_e + \hat{e} \overline{(Cont.-FS2)^{1t}}, \tag{184}$$

$$\begin{aligned} (Skew.-FS2)_e &= \frac{1}{2} (Div.-FS2)_e + \frac{1}{2} (Adv.-FS2)_e = (Div.-FS2)_e - \frac{1}{2} \hat{e} \overline{(Cont.-FS2)^{1t}} \\ &= (Adv.-FS2)_e + \frac{1}{2} \hat{e} \overline{(Cont.-FS2)^{1t}}, \end{aligned} \tag{185}$$

$$\hat{e} (Skew.-FS2)_e = \frac{\delta_1 \overline{\bar{\rho}^{1t}} e^2 / 2}{\delta_1 t} + \frac{1}{J} \frac{\delta_1 \overline{G_j^{-1t} \hat{e} \hat{e}^{1\zeta_j}}}{\delta_1 \zeta_j} / 2. \tag{186}$$

The convective term of the corresponding discrete total energy equation is

$$\frac{1}{J} \overline{\hat{u}_i J^{1\zeta_i} (Skew.-FS2)_i} + (Div.-FS2)_e = \frac{\delta_1 (\rho E)_{FS2}}{\delta_1 t} + \frac{1}{J} \frac{\delta_1}{\delta_1 \zeta_j} \left(\frac{1}{2} \overline{G_j^{-1t} \zeta_j} \widehat{u}_i \widehat{u}_i^{1\zeta_j} + \overline{G_j^{-1t} \bar{e}^{1\zeta_j}} \right), \tag{187}$$

where conserved discrete total energy norm, $(\rho E)_{FS2}$, is

$$(\rho E)_{FS2} \equiv \frac{1}{2} \frac{1}{J} \overline{J \bar{\rho}^{1t} \zeta_i^{-1}} u_i u_i + \overline{\bar{\rho}^{1t}} e. \tag{188}$$

Conservation properties of the pressure and viscous terms in the discrete total energy equation are also demonstrated as follows:

$$\frac{1}{J} \overline{\widehat{u}_i J^{1\zeta_i} (\text{Pres.-FS2})_i}^{-1\zeta_i} + (\text{PD.-FS2})_e = \frac{1}{J} \frac{\delta_1}{\delta_1 \zeta_i} \left\{ \left(\frac{J}{\widehat{h}_i} \widehat{u}_i \right) \overline{\overline{\overline{p^{1t}}}}^{1\zeta_i} \right\}, \tag{189}$$

$$\frac{1}{J} \widehat{u}_i J^{1\zeta_i} \left\{ \frac{1}{\overline{\overline{\overline{1}}}}^{-1\zeta_i} \frac{\delta_1}{\delta_1 \zeta_j} \odot \left(\frac{J}{\widehat{h}_j} \tau_{ij} \right) \right\}^{-1\zeta_i} + \frac{1}{J} \tau_{ij} \odot \left(\frac{J}{\widehat{h}_j} \frac{\delta_1 \widehat{u}_i}{\delta_1 \zeta_j} \right) = \frac{1}{J} \frac{\delta_1}{\delta_1 \zeta_j} \left\{ \widehat{u}_i \odot \left(\frac{J}{\widehat{h}_j} \tau_{ij} \right) \right\}, \tag{190}$$

where

$$\frac{\delta_1}{\delta_1 \zeta_j} \odot \left(\frac{J}{\widehat{h}_j} \tau_{1j} \right) \equiv \frac{\delta_1 (\widehat{h}_2 \widehat{h}_3 \tau_{11})}{\delta_1 \zeta_1} + \frac{\delta_1 (\overline{\widehat{h}_1}^{-1\zeta_1} \widehat{h}_3 \tau_{12})}{\delta_1 \zeta_2} + \frac{\delta_1 (\overline{\widehat{h}_1}^{-1\zeta_1} \widehat{h}_2 \tau_{13})}{\delta_1 \zeta_3}, \tag{191}$$

$$\frac{\delta_1}{\delta_1 \zeta_j} \odot \left(\frac{J}{\widehat{h}_j} \tau_{2j} \right) \equiv \frac{\delta_1 (\overline{\widehat{h}_2}^{-1\zeta_2} \widehat{h}_3 \tau_{21})}{\delta_1 \zeta_1} + \frac{\delta_1 (\widehat{h}_1 \widehat{h}_3 \tau_{22})}{\delta_1 \zeta_2} + \frac{\delta_1 (\widehat{h}_1 \overline{\widehat{h}_2}^{-1\zeta_2} \tau_{23})}{\delta_1 \zeta_3}, \tag{192}$$

$$\frac{\delta_1}{\delta_1 \zeta_j} \odot \left(\frac{J}{\widehat{h}_j} \tau_{3j} \right) \equiv \frac{\delta_1 (\widehat{h}_2 \widehat{h}_3^{-1\zeta_3} \tau_{31})}{\delta_1 \zeta_1} + \frac{\delta_1 (\widehat{h}_1 \overline{\widehat{h}_3}^{-1\zeta_3} \tau_{32})}{\delta_1 \zeta_2} + \frac{\delta_1 (\widehat{h}_1 \widehat{h}_2 \tau_{33})}{\delta_1 \zeta_3}, \tag{193}$$

$$\tau_{ij} \odot \left(\frac{J}{\widehat{h}_j} \frac{\delta_1 \widehat{u}_i}{\delta_1 \zeta_j} \right) \equiv \left(\tau_{11} \widehat{h}_2 \widehat{h}_3 \frac{\delta_1 \widehat{u}_1}{\delta_1 \zeta_1} + \tau_{22} \widehat{h}_1 \widehat{h}_3 \frac{\delta_1 \widehat{u}_2}{\delta_1 \zeta_2} + \tau_{33} \widehat{h}_1 \widehat{h}_2 \frac{\delta_1 \widehat{u}_3}{\delta_1 \zeta_3} \right) + \tau_{12} \left(\overline{\widehat{h}_1}^{-1\zeta_1} \widehat{h}_3 \frac{\delta_1 \widehat{u}_1}{\delta_1 \zeta_2} + \overline{\widehat{h}_2}^{-1\zeta_2} \widehat{h}_3 \frac{\delta_1 \widehat{u}_2}{\delta_1 \zeta_1} \right) \tag{194}$$

$$+ \tau_{13} \left(\overline{\widehat{h}_1}^{-1\zeta_1} \widehat{h}_2 \frac{\delta_1 \widehat{u}_1}{\delta_1 \zeta_3} + \overline{\widehat{h}_3}^{-1\zeta_3} \widehat{h}_2 \frac{\delta_1 \widehat{u}_3}{\delta_1 \zeta_1} \right) + \tau_{23} \left(\overline{\widehat{h}_1}^{-1\zeta_1} \overline{\widehat{h}_2}^{-1\zeta_2} \frac{\delta_1 \widehat{u}_2}{\delta_1 \zeta_3} + \overline{\widehat{h}_3}^{-1\zeta_3} \overline{\widehat{h}_2}^{-1\zeta_2} \frac{\delta_1 \widehat{u}_3}{\delta_1 \zeta_2} \right),$$

$$\frac{\delta_1}{\delta_1 \zeta_j} \left\{ \widehat{u}_i \odot \left(\frac{J}{\widehat{h}_j} \tau_{ij} \right) \right\} \equiv \frac{\delta_1 \left(\overline{\widehat{u}_1} (\widehat{h}_2 \widehat{h}_3 \tau_{11})^{-1\zeta_1} + \overline{\widehat{u}_2}^{-1\zeta_1} \overline{\widehat{h}_2}^{-1\zeta_2} \widehat{h}_3 \tau_{12} + \overline{\widehat{u}_3}^{-1\zeta_1} \widehat{h}_2 \overline{\widehat{h}_3}^{-1\zeta_3} \tau_{13} \right)}{\delta_1 \zeta_1}$$

$$+ \frac{\delta_1 \left(\overline{\widehat{u}_1}^{-1\zeta_2} \overline{\widehat{h}_1}^{-1\zeta_1} \widehat{h}_3 \tau_{21} + \widehat{u}_2 (\widehat{h}_1 \widehat{h}_3 \tau_{22})^{-1\zeta_2} + \overline{\widehat{u}_3}^{-1\zeta_2} \widehat{h}_1 \overline{\widehat{h}_3}^{-1\zeta_3} \tau_{23} \right)}{\delta_1 \zeta_2}$$

$$+ \frac{\delta_1 \left(\overline{\widehat{u}_1}^{-1\zeta_3} \overline{\widehat{h}_1}^{-1\zeta_1} \widehat{h}_2 \tau_{31} + \overline{\widehat{u}_2}^{-1\zeta_3} \widehat{h}_1 \overline{\widehat{h}_2}^{-1\zeta_2} \tau_{32} + \widehat{u}_3 (\widehat{h}_1 \widehat{h}_2 \tau_{33})^{-1\zeta_3} \right)}{\delta_1 \zeta_3}.$$

Therefore, the fully discrete finite difference schemes for a non-uniform staggered grid system presented in this appendix are fully conservative.

The discrete internal energy equation and corresponding state equation can be replaced by the following ones when enthalpy [18] is preferable to internal energy:

$$(\text{Conv.-FS2})_h - (\text{DpDt.} - \text{FS2})_h = \frac{1}{J} \tau_{ij} \odot \left(\frac{J}{\widehat{h}_j} \frac{\delta_1 \widehat{u}_i}{\delta_1 \zeta_j} \right) - \frac{1}{J} \frac{\delta_1}{\delta_1 \zeta_j} \left(\frac{J}{\widehat{h}_j} q_j \right), \tag{196}$$

$$\text{with } \overline{p^{1t}} = p(\overline{p^{1t}}, h), \quad \text{or } \overline{\rho^{1t}} = \rho(\overline{p^{1t}}, h), \quad \text{or } h = h(\overline{p^{1t}}, \overline{p^{1t}}). \tag{197}$$

$(\text{Conv.-FS2})_h$ is a generic form of convective term in the discrete enthalpy equation and takes the same form for $(\text{Conv.-FS2})_e$, where e is replaced by h . $(\text{DpDt.} - \text{FS2})_h$ is the discrete material derivative of pressure in the enthalpy equation:

$$(\text{DpDt.} - \text{FS2})_h \equiv \frac{\delta_1 \overline{p^{1t}}}{\delta_1 t} + \frac{1}{J} \left(\frac{J}{\widehat{h}_i} \widehat{u}_i \right) \frac{\delta_1 \overline{p^{1t}}}{\delta_1 \zeta_i} \tag{198}$$

The inviscid part of the total energy equation with the enthalpy scheme is written as

$$\left\{ \frac{1}{J} \widehat{u}_i J^{1\zeta_i} (\text{Skew.-FS2})_i^{-1\zeta_i} + (\text{Div.-FS2})_h \right\} + \left\{ \frac{1}{J} \widehat{u}_i J^{1\zeta_i} (\text{Pres.-FS2})_i^{-1\zeta_i} - (\text{PD.-FS2})_h \right\}$$

$$= \frac{\delta_1 (\rho E)_{\text{FS2}}^h}{\delta_1 t} + \frac{1}{J} \frac{\delta_1}{\delta_1 \zeta_j} \left(\frac{1}{\overline{\overline{\overline{G_j}}}}^{-1\zeta_i} \widehat{u}_i \widehat{u}_j^{-1\zeta_j} + \overline{\overline{\overline{G_j}}^{1t}} \overline{\overline{\overline{h}}}^{-1\zeta_j} \right), \tag{199}$$

where $(\rho E)_{\text{FS2}}^h$ is the discrete total energy norm conserved by the second-order accurate scheme with enthalpy:

$$(\rho E)_{\text{FS2}}^h \equiv \frac{1}{2} \frac{1}{J} \overline{\overline{\overline{p^{1t}}}}^{-1\zeta_i} u_i u_i + \overline{p^{1t}} h - \overline{p^{1t}}. \tag{200}$$

This indicates that the fully discrete enthalpy scheme discretely conserves the total energy norm and is also fully conservative.

References

- [1] Y. Morinishi, T.S. Lund, O.V. Vasilyev, P. Moin, Fully conservative higher order finite difference schemes for incompressible flow, *J. Comput. Phys.* 143 (1998) 90–124.
- [2] F.H. Harlow, J.E. Welch, Numerical calculation of time-dependent viscous incompressible flow of fluid with free surface, *Phys. Fluids* 8 (1965) 2182–2189.
- [3] O.V. Vasilyev, High order finite difference schemes on non-uniform meshes with good conservation properties, *J. Comput. Phys.* 157 (2000) 746–761.
- [4] Y. Morinishi, O.V. Vasilyev, T. Ogi, Fully conservative finite difference scheme in cylindrical coordinates for incompressible flow simulations, *J. Comput. Phys.* 197 (2004) 686–710.
- [5] R.W.C.P. Verstappen, A.E.P. Veldman, Symmetry-preserving discretization of turbulent flow, *J. Comput. Phys.* 187 (2003) 343–368.
- [6] F. Nicoud, Conservative high-order finite-difference schemes for low-Mach number flows, *J. Comput. Phys.* 158 (2000) 71–97.
- [7] O. Desjardins, G. Blanquart, G. Balarac, H. Pitsch, High order conservative finite difference scheme for variable density low Mach number turbulent flows, *J. Comput. Phys.* 227 (2008) 7125–7159.
- [8] A.G. Kravchenko, P. Moin, On the effect of numerical errors in large eddy simulations of turbulent flows, *J. Comput. Phys.* 131 (1997) 310–322.
- [9] C.A. Kennedy, A. Gruber, Reduced aliasing formulations of the convective terms within the Navier–Stokes equations for a compressible fluid, *J. Comput. Phys.* 227 (2008) 1676–1700.
- [10] W.J. Feiereisen, W.C. Reynolds, J.H. Ferziger, Numerical Simulation of Compressible, Homogeneous Turbulent Shear Flow, Department Mechanical Engineering, Stanford University, Report No. TF-13, 1981.
- [11] G.A. Blaisdell, N.N. Mansour, W.C. Reynolds, Numerical Simulations of Compressible Homogeneous Turbulence, Stanford University, Report No. TF-50, 1991.
- [12] G.A. Blaisdell, N.N. Mansour, W.C. Reynolds, Compressibility effects on the growth and structure of homogeneous turbulent shear flow, *J. Fluid Mech.* 256 (1993) 443–485.
- [13] F. Ducros, V. Ferrand, F. Nicoud, C. Weber, D. Darracq, C. Gacherieu, T. Poinot, Large-eddy simulation of the shock/turbulence interaction, *J. Comput. Phys.* 152 (1999) 517–549.
- [14] F. Ducros, F. Laporte, T. Soulères, V. Guinot, P. Moinat, B. Caruelli, High-order fluxes for conservative skew-symmetric-like schemes in structured meshes: application to compressible flows, *J. Comput. Phys.* 161 (2000) 114–139.
- [15] Y. Morinishi, S. Tamano, K. Nakabayashi, A DNS algorithm using B-spline collocation method for compressible turbulent channel flow, *Comput. Fluids* 32 (2003) 751–776.
- [16] F.E. Ham, F.S. Lien, A.B. Strong, A fully conservative second-order finite difference scheme for incompressible flow on nonuniform grids, *J. Comput. Phys.* 177 (2002) 117–133.
- [17] C.D. Pierce, Progress-variable Approach for Large-eddy Simulation of Turbulent Combustion, Ph.D. Thesis, Stanford University, Stanford, CA, 2001.
- [18] C. Wall, C.D. Pierce, P. Moin, A semi-implicit method for resolution of acoustic waves in low Mach number flows, *J. Comput. Phys.* 181 (2002) 545–563.
- [19] A.E. Honein, P. Moin, Higher entropy conservation and numerical stability of compressible turbulence simulations, *J. Comput. Phys.* 201 (2004) 531–545.
- [20] Y. Morinishi, Secondary conservative finite difference scheme of convection for compressible turbulent flow analysis, in: *Proceedings of the 22nd SEIKEN TSFD Symposium, Tokyo, 2007*, pp. 69–75 (in Japanese).
- [21] P.K. Subbareddy, G.V. Candler, A fully discrete, kinetic energy consistent finite-volume scheme for compressible flows, *J. Comput. Phys.* 228 (2009) 1347–1364.
- [22] P. Roe, Approximated Riemann solvers, parameter vectors, and difference schemes, *J. Comput. Phys.* 43 (1981) 357–372.
- [23] S.K. Lele, Compact finite difference schemes with spectral-like resolution, *J. Comput. Phys.* 103 (1992) 16–42.
- [24] S. Nagarajan, S.K. Lele, J.H. Ferziger, A robust high-order compact method for large eddy simulation, *J. Comput. Phys.* 191 (2003) 392–419.
- [25] J.H. Williamson, Low-storage Runge–Kutta schemes, *J. Comput. Phys.* 35 (1980) 48–56.
- [26] D.A. Knoll, D.E. Keyes, Jacobian-free Newton–Krylov methods: a survey of approaches and applications, *J. Comput. Phys.* 193 (2004) 357–397.
- [27] P.N. Brown, Y. Saad, Hybrid Krylov methods for nonlinear systems of equations, *SIAM J. Sci. Stat. Comput.* 11 (1990) 450–481.
- [28] Y. Saad, M.H. Schultz, GMRES: a generalized minimal residual algorithm for solving nonsymmetric linear systems, *SIAM J. Sci. Stat. Comput.* 7 (1986) 856–869.
- [29] Y. Saad, A flexible inner-outer preconditioned GMRES algorithm, *SIAM J. Sci. Stat. Comput.* 14 (1993) 461–469.
- [30] R. Samtaney, D.I. Pullin, B. Kosović, Direct numerical simulation of decaying compressible turbulence and shocklet statistics, *Phys. Fluids* 13 (2001) 1415–1430.
- [31] N.K. Ghaddar, K.Z. Korczak, B.B. Mikic, A.T. Patera, Numerical investigation of incompressible flow in grooved channels. Part 1. Stability and self-sustained oscillations, *J. Fluid Mech.* 163 (1986) 99–127.
- [32] Y. Morinishi, Forms of convection and quadratic conservative finite difference schemes for low-Mach number compressible flow simulations, *Trans. JSME* 73 (Series B) (2007) 451–458 (in Japanese).
- [33] M. Vinokur, Conservation equations of gasdynamics in curvilinear coordinate systems, *J. Comput. Phys.* 14 (1974) 105–125.